

Spatial population structure determines extinction risk in climate-induced range shifts

Manuscript elements: Figure 1, figure 2, figure 3, online appendices A and B (including figures ~~A1&A2~~A1-A3, tables ~~A1&A2~~A1-A4, and figures B1-B11). Figure 1 and figure 3 are to print in color.

Keywords: range shifts, ~~eco-evolutionary dynamics~~, ~~local adaptation~~, extinction, rapid evolution, dispersal evolution, individual-based model

Manuscript type: Article.

Prepared using the suggested L^AT_EX template for *Am. Nat.*

Abstract

Climate change is an ~~increasingly severe~~ escalating threat facing populations around the globe, necessitating a robust understanding of the ecological and evolutionary mechanisms dictating population responses. ~~Population dynamics of range shifts, among the most commonly observed responses~~ However, populations do not respond to climate change ~~, can be influenced by many factors, including evolution of key traits, the degree of local adaptation, and the nature of the range edge~~ in isolation, but rather in the context of their existing ranges. In particular, spatial population structure within a range (e.g. trait clines, starkness of range edges, etc.) likely interacts with other ecological and evolutionary processes during climate-induced range shifts. Here, we use an individual-based model to explore the interacting roles of these factors in ~~the dynamics of climate-induced range shifts~~ range shifts dynamics. We show that ~~aspects of~~ the spatial population structure ~~within the initial range~~, in particular the ~~potential for local adaptation~~ slope of the gradient in a trait optimum, severely increased a population's extinction risk. Further, and contrary to expectations, we show that evolution of heightened dispersal during range shifts was unable to rescue faltering populations. Rather, a population's fate during climate change was determined by the composition of dispersal phenotypes ~~that evolved within the initial range~~ defining the population at equilibrium (i.e. before the onset of rapid climate change); only populations consisting of highly dispersive individuals ~~prior to the onset of climate change~~ survived. Our results demonstrate that dispersal evolution alone may be insufficient to save a range shifting population and that ~~initial spatial population structure plays a pivotal role in determining the outcome of climate-induced~~ can substantially increase extinction risk in range shifts.

Introduction

Climate change is expected to dramatically reshape global biogeographic patterns as some species
24 shift their ranges to track changing environmental conditions (Gonzalez et al., 2010). These range
shifts are generally predicted to proceed upwards in latitude, elevation, or both as average global
temperatures continue to rise (Loarie et al., 2009). Indeed, contemporary range shifts have already
27 been observed in a wide variety of taxa, ranging from algae to mammals (Chen et al., 2011; Parme-
san, 2006). Such range shifts present significant challenges to current and future conservation
efforts as they can result in the extinction of populations failing to track a changing climate (Parme-
30 san, 2006) as well as the creation of novel species assemblages (Hobbs et al., 2009). Understanding
the ecological and evolutionary dynamics of such climate-induced range shifts will play a key role
in informing current and future conservation work.

33 Large-scale population movements have been studied for decades in the context of range ex-
pansions (e.g. of invasive or reintroduced species), leading to a robust understanding of both the
ecological (Hastings et al., 2005) and evolutionary (Excoffier et al., 2009; Shine et al., 2011)
36 mechanisms shaping such expansions. For example, while the speed of a range expansion can
be well approximated by a combination of the species' intrinsic growth rate and dispersal abil-
ity (~~Hastings et al., 2005~~)(Fisher, 1937; Hastings et al., 2005), recent research demonstrates that
39 evolution in both of these traits can increase both the mean and variance of expansion speed through
time (Ochocki and Miller, 2017; Phillips, 2015; Shaw and Kokko, 2015; Szűcs et al., 2017; Weiss-
Lehman et al., 2017). As fundamentally similar spatial processes, it is likely that range shifts
42 will also be subject to these ecological and evolutionary mechanisms known to drive range expan-
sions. However, range shifts involve several additional complications absent from range expan-
sions, which must be considered when predicting the dynamics of a shifting population. In par-

45 ticular, range shifts ~~occur in populations begin~~ with far more complex spatial population structure
compared to most range expansions, ~~which typically begin from the successful establishment and~~
~~spread of a small, founding population~~ (Hastings et al., 2005). While these founding populations
48 ~~often lack any significant spatial structure, populations undergoing range shifts are characterized~~
~~by a~~. Here and throughout the paper, we use the phrase spatial population structure to refer broadly
to the spatial distribution of individuals, and their associated genotypes and phenotypes, within a
51 population. Thus, spatial population structure can encompass factors such as spatial clines in trait
values and the starkness of abundance declines characterizing the range edge. Range expansions
(e.g. of invasive or reintroduced species) typically start from small founding populations brought
54 to a new area and lacking any initial spatial population structure. While such populations form
spatial population structure ~~formed by aspects of the previously stable ranges~~ during the expansion
process (Ochocki and Miller, 2017; Weiss-Lehman et al., 2017), established populations respond
57 to climate change in the context of preexisting spatial population structure. For example, popu-
lation ranges can vary in ~~their potential for local adaptation throughout the range, the nature the~~
presence and severity of gradients in trait optima, the starkness of the range edge, and, thus, the
60 spatial distribution of key traits.

Each of these factors relating to spatial population structure has the potential to affect the
dynamics of range shifts under changing climatic conditions. For example, the underlying mecha-
63 nism ~~responsible for the gradient in population size from the range core to the~~ causing population
declines at the range edge (i.e. declines in carrying capacity versus growth rate) ~~alters~~ can alter
a population's extinction risk during climate driven range shifts (Henry et al., 2013). Further, in
66 ranges characterized by a gradient in a trait optimum, the starkness of the range edge can impact
the ability of peripheral populations to adapt to the local optimum, with stark range edges leading
to better adaptation in peripheral populations (García-Ramos and Kirkpatrick, 1997), though the

69 importance of this for range shifts has not been investigated. Additionally, ~~the potential for local~~
~~adaptation throughout a range has been related to extinction risk during range shifts . Specifically, a~~
~~low potential for local adaptation can decrease a population's ability to track a changing climate if~~
72 the nature of dispersal can interact with adaptation to a gradient in a trait optimum to impact range
shift dynamics. When dispersal occurs in a stepping stone manner, ~~allowing some individuals to~~
~~maladapted individuals (i.e. individuals whose phenotypes do not match the local optimum) can~~
75 block the establishment of better adapted genotypes so long as the mismatch is not too severe (Atkins
and Travis, 2010). While these aspects of spatial population structure have been shown to impact
the dynamics of climate-induced range shifts in isolation, it is unclear how and if they might inter-
78 act.

Further, given the importance of rapid trait evolution in range expansions (Ochocki and Miller,
2017; Phillips, 2015; Shaw and Kokko, 2015; Szűcs et al., 2017; Weiss-Lehman et al., 2017), it is
81 necessary to consider the interplay between aspects of spatial population structure and the role of
rapid evolution during range shifts. In asexual species, for example, local adaptation to a gradient
in a trait optimum has been shown to interact with dispersal evolution during climate change,
84 driving increased dispersal probability as genotypes shift to keep pace with their environmental
optimum (Hargreaves et al., 2015). However, it is unclear how these two processes might interact
in a sexually reproducing species in which dispersal and local adaptation are directly linked via
87 gene flow. Under sexual reproduction, evolution of increased dispersal could simultaneously re-
duce local adaptation to a gradient in a trait optimum within a population due to increased gene
flow throughout the range (García-Ramos and Kirkpatrick, 1997; Kirkpatrick and Barton, 1997).
90 In fact, long-distance pollen dispersal in flowering plants has been shown to restrict local adap-
tation and, when pollen dispersal sufficiently outpaces seed dispersal, to lead to ecological niche
shifts, rather than spatial range shifts, in response to simulated climate change (Aguilée et al.,

93 2016). In addition to potential interactions between local adaptation and dispersal evolution, the ~~nature~~ starkness of the range edge could influence the potential for rapid trait evolution during range shifts ~~. For example, the severity of the environmental gradient forming the range edge has~~
96 ~~been shown to alter the~~ by altering the spatial distribution of dispersal phenotypes throughout the range (Hargreaves and Eckert, 2014; Henry et al., 2013), thus altering the diversity of dispersal genotypes present for subsequent evolution during range shifts.

99 Here, we assess the interaction of ~~multiple aspects of~~ two mechanisms responsible for spatial population structure with trait evolution in sexually reproducing populations undergoing ~~climate-induced~~ range shifts. We develop an individual-based model capable of ~~incorporating~~ producing a wide va-
102 riety of spatial population structures in which males and females are defined by two genetically determined traits, thus allowing for both evolutionary and ecological responses to climate change. One trait determines dispersal ability while the second defines an individual's environmental niche.
105 Using this model, we vary both the ~~potential for local adaptation within the range and the nature severity of the gradient in the niche optimum and the starkness~~ of the range edge to ascertain how they interact with each other and with the process of trait evolution to impact a population's ability
108 to track a changing climate. ~~By~~ Additionally, by contrasting the dynamics of extant and extinct populations, we isolate the factors most strongly contributing to extinction risk during climate change.

111 Methods

A full description of the individual-based model using the Overview, Design concepts, and Details protocol (Grimm et al., 2010) is available in Appendix A, while we present a brief summary here.
114 Population dynamics occurred within discrete habitat patches embedded in a two dimensional lattice in which environmental conditions varied along the x dimension but remained constant along

the y dimension (Fig. A1). Landscapes were unbounded in the x dimension but defined by a
 117 fixed width and wrapping boundaries in the y dimension. The optimum environmental niche value
changed linearly along the x dimension, thus allowing for the intrinsic formation of stable range
boundaries when the optimum changed rapidly enough (Alleaume-Benharira et al., 2006; Kirkpatrick and Barton, 1997;
 120 However, to examine the dynamics of ranges in which the niche optimum does not change rapidly
enough to form stable range limits, we additionally imposed extrinsic range limits to prevent
continuous adaptation and spread of the population (Alleaume-Benharira et al., 2006; García-Ramos and Kirkpatrick, 19
 123 Specifically, we systematically altered the decline in patch carrying capacities from the range core
to the edge (Alleaume-Benharira et al., 2006; Bocedi et al., 2014; Henry et al., 2013; Mustin et al., 2009) in
such a way that we could directly manipulate the starkness of the decline. Previous research has
 126 shown that using a decline in intrinsic growth rate as opposed to carrying capacity may impact
extinction risk but does not alter the patterns of dispersal evolution during climate change (Henry et al., 2013).
To maintain generality, we do not assume a specific mechanism behind the decline in carrying
 129 capacity, but it could represent a variety of range limiting mechanisms such as physiological limits
to adaptation, the effects of competition, or underlying resource distributions (Case and Taper, 2000; Holt et al., 2005; Se
 Thus, the x dimension defined the environmental context of the population and the y dimension al-
 132 lowed for variation in population dynamics under identical environmental conditions. To simulate
 climate change, ~~environmental conditions~~ the patch carrying capacities and the gradient in the niche
optimum shifted at a constant rate along the x dimension. Generations were non-overlapping and
 135 consisted of discrete dispersal and reproduction phases (Fig. A2).

Individuals were characterized by two traits (dispersal and an environmental niche), both de-
 fined by a set of 5 quantitative diploid loci. While the number of loci was arbitrary, 5 was chosen as
 138 a compromise between computational restrictions and the likely polygenic nature of such complex
 traits. The dispersal trait defined an individual's expected dispersal distance, assuming an expo-

nential dispersal kernel. An individual's ~~environmental niche value allowed for local adaptation;~~
141 ~~the closer the niche value to the environmental optimum of the~~ realized dispersal distance was
~~then drawn from the dispersal kernel and dispersal direction was random and unbiased. Dispersal~~
~~occurred in continuous space from the center of an individual's patch, the higher the current patch~~
144 ~~and the individual's realized fitness. The environmental optimum of individual patches could then~~
~~be systematically varied across the range to allow for different degrees of local adaptation (i. e.~~
~~larger changes in environmental optima allowed for greater local adaptation of the population). In~~
147 ~~addition to the potential for local adaptation, simulated ranges were characterized by a decline~~
~~in patch carrying capacity from the range center to the edge, the severity of which could be~~
~~adjusted without altering the total carrying capacity of the landscape (see Appendix A)~~ new patch
150 was then determined by the mapping from continuous space to discrete patches (see Appendix
A). An individual's environmental niche value determined its fitness according to the local niche
optimum. The closer an individual's niche value to the local environmental optimum, the higher
153 the individual's realized fitness. Reproduction within each patch occurred via a stochastic imple-
mentation of the classic Ricker model (Melbourne and Hastings, 2008; Ricker, 1954), scaled by
the mean fitness of the patch. Parental pairs formed via random sampling of the local population
156 (with replacement) weighted by individual fitness ~~—such that individuals with a close match of~~
~~their niche value to the local optimum produced more offspring on average. Thus, the model used~~
~~a mixture of hard selection (realized population growth declines with maladaptation relative to the~~
159 ~~niche optimum) and soft selection (probability of producing offspring depends on fitness relative~~
~~to other individuals) for the evolutionary dynamics (Wallace, 1975).~~ Allele inheritance was subject
to mutation and assumed no linkages among loci. The mutation process was designed such that
162 mutational input per generation was independent of the number of loci (see Appendix A) and with
parameters corresponding to previous estimates from the literature (Gilbert et al., 2017).

To determine the effect of spatial population structure on the eco-evolutionary dynamics of
 range shifts, we varied parameter combinations. We varied parameter values to explore the interact-
 ing roles of local adaptation and the severity of the gradient in environmentally suitable habitat at
 the niche optimum and the starkness of the range edge (Table A1 and A2) in forming spatial
 population structure at equilibrium and driving the subsequent eco-evolutionary dynamics of range
 shifts. Specifically, we considered a factorial combination of three experimental factors: (1) no,
 low, and high potential for local adaptation; a flat, shallow, and steep gradient in the niche optimum
 across space; (2) shallow, moderate, and stark gradients in suitable habitat declines in carrying
 capacity at the range edge, and (3) slow, moderate, and fast speeds of climate change. This yielded
 a total of 27 different scenarios, each explored with 200 simulations. Each simulation ran for 2150
 generations with stable climate conditions for the first 2000 to reach a spatial equilibrium, fol-
 lowed by 100 generations of climate change and a final 50 generations of stable conditions. Figure
 1 shows an example of a single population responding to a moderate speed of climate change. For
 each scenario, we evaluated the role of dispersal evolution and initial the equilibrium spatial popu-
 lation structure in driving and dispersal evolution in the dynamics of the range shifting populations.
 We primarily discuss simulations using assuming a moderate speed of climate change in the main
 text, but present the results for slow and fast speeds of climate change in Appendix B.

We calculated dispersal evolution in each patch throughout the landscape as the change in
 mean dispersal phenotype from the beginning of the period of climate change to the end. For this
 analysis, we defined individual patches by their relative location within the range rather than with
 their fixed spatial coordinates (e.g. leading edge vs. core populations). Due to local extinctions,
 not all patches were occupied at the end of the period of climate change. To quantify dispersal
 evolution in these patches, we used data from the last generation in which the population had at
 least 10 individuals. Changes in mean dispersal phenotype were calculated by subtracting the initial

mean dispersal phenotype from the value at the end of climate change (or at the last generation of
189 at least 10 individuals occupying the patch in the case of population extinctions); positive values
indicate an increase in the mean dispersal phenotype. All simulations and data processing were
performed in R version 3.4.4 (Team, 2000) and the code is available at (links are available from the
192 journal office).

Results

In all scenarios, some populations shifted their ranges in response to climate change. However the
195 proportion of extinct populations that failed to track the changing climate depended on the ~~initial~~
~~spatial population structure~~spatial characteristics of the range. Populations defined by a ~~higher~~
~~potential for local adaptation~~steep gradient in the niche optimum and by stark ~~habitat gradients~~
198 declines in carrying capacity at the range edge experienced the greatest probability of extinction
due to climate change (quantified by the proportion of simulated populations to go extinct through
time; Fig. 2). While both aspects of a population's range influenced extinction probabilities, the
201 ~~potential for local adaptation~~gradient in the niche optimum drove more dramatic changes to ex-
tinction risk, with ~~greater changes in environmental optima across the landscape~~steeper gradients
causing severe increases in the probability of extinction during climate change. We varied both
204 parameters widely (the ~~potential for local adaptation~~slope of the gradient in the niche optimum
doubled from the ~~low to high~~shallow to steep scenario and the parameter defining the ~~severity~~
~~of the environmental gradient~~starkness of the range edge was increased by a factor of ~~100~~100
207 from shallow to stark ~~gradients~~edges; Table A2), suggesting that ~~potential for local adaptation~~the
gradient in the niche optimum may be the stronger driver of extinction risk during climate-induced
range shifts across a wide region of parameter space and corresponding biological scenarios. Ad-
210 ditionally, as expected, the pace of climate change also influenced extinction probabilities with

faster climate change corresponding to greater extinction risk (Fig. B1 & B2). However, this effect was independent of the ~~roles of local adaptation and the habitat gradient at~~ gradient in the niche optimum and the starkness of the range edge in determining ~~the~~ extinction probability during ~~a~~ range shift ~~range shifts~~.

In accordance with previous results, populations at the range edge had lower fitness than central
populations at equilibrium and this effect was amplified with more gradual range edges (García-Ramos and Kirkpatrick,
Counterintuitively, populations that survived climate change tended to be characterized by ~~reduced~~
even greater reductions in fitness at the range ~~margins prior to the onset of climate change~~ edges at
equilibrium compared to populations that went extinct (Fig. B3-B5). ~~Essentially, populations with~~
~~initially higher degrees of local adaptation at the range edges, and thus greater fitness, were more~~
~~likely to go extinct during climate change. This~~ While discernible in all simulations with a non-zero
slope in the gradient of the niche optimum, this pattern was most evident in the ~~simulations with~~
~~either (1) a gradual environmental gradient at the range edge or (2) a high potential for local~~
~~adaptation~~ scenarios defined by a gradual range edge. As expected, there was no spatial varia-
tion in fitness for populations with no ~~potential for local adaptation.~~ variation in the niche optimum
across space. Despite the spatial variation in fitness in some scenarios, variance in relative fitness
within a patch was relatively low (about 0.3 across all scenarios). This implies that (1) the reduction
in fitness at the edge caused by the spatial gradient in the niche optimum was relatively uniform
across all individuals, and (2) as a result, there was relatively low variance in reproductive success
in these populations, meaning that evolution at the edge was not driven by only a handful of higher
fitness individuals.

Dispersal evolution is predicted to play a key role in aiding populations as they shift to track a changing climate. While some ~~individual~~ simulations confirmed these expectations with average
dispersal phenotypes increasing through time (e.g. Fig. 1), examining all simulations from each

experimental scenario revealed no differences in the magnitude or direction of dispersal evolution between successful and extinct populations (Fig. 3a&b). Populations in all parameter combinations experienced both increases and decreases in average dispersal phenotypes, with all distributions of observed changes in dispersal phenotypes centered on 0 (Fig. B3-B5). Further, calculating the coefficient of variation (CV) in dispersal genotypes over the y dimension, in which environmental conditions did not vary, revealed that edge populations had between 3 and 4 times higher CVs than core populations across all scenarios, indicating genetic diversity at the edge was not a limiting factor in dispersal evolution. The similarity in evolved changes in dispersal between surviving and extinct populations suggests that dispersal evolution alone cannot explain which populations successfully tracked moving conditions and which became extinct.

Instead, the initial distribution of dispersal phenotypes prior to the onset of climate change at equilibrium played a key role in determining a population's fate. A range of dispersal phenotypes evolved in populations over the 2000 generations of stable climatic conditions in response to the potential for local adaptation and the severity of the habitat gradient at the gradient in the niche optimum and the starkness of the range edge (Fig. B9-B11). Populations that survived climate change were composed primarily of individuals with heightened dispersal phenotypes (Fig. 3c&d). In fact, comparing Previous research has demonstrated that defining the range edges via a decline in the intrinsic growth rate (as opposed to carrying capacity as done here) resulted in less dispersive phenotypes at the range edge (Henry et al., 2013), meaning extinction risks would be even higher under such a scenario. Comparing the full distribution of initial equilibrium dispersal phenotypes present in a given experimental scenario to the distribution of phenotypes just from surviving populations revealed a threshold value delineating individuals from surviving versus extinct populations. Comparison of the different experimental scenarios revealed this threshold to be constant for a given speed of climate change (Fig. B9-B11). To explain this

phenomenon, we used the well-known approximation for the speed of an expanding population, $2\sqrt{rD}$ (~~Hastings et al., 2005~~)([Fisher, 1937; Hastings et al., 2005](#)), in which r is the intrinsic growth rate and D is the diffusion coefficient, to calculate the dispersal phenotype necessary to produce an expansion wave exactly matching the speed of climate change ~~used~~ in our simulations (see the model description in Appendix A). This [estimated](#) dispersal phenotype matched the observed threshold value distinguishing surviving from extinction populations in all experimental scenarios (Figures B9-B11, vertical dashed line). Thus, surviving populations in each scenario happened to be the lucky few already composed primarily of individuals with dispersal phenotypes capable of spreading at the pace of climate change, rather than populations in which heightened dispersal evolved over time in response to climate change. [However, this threshold effect weakened slightly in scenarios with a slow speed of climate change indicating a potential role for dispersal evolution if the climate were to change at a slow enough rate \(Figure B11\).](#)

Discussion

Range shifts due to climate change represent a global threat to biodiversity and much recent research has focused on exploring the underlying ecological and evolutionary dynamics of such range shifts to inform conservation efforts. We developed an individual-based model to explore the eco-evolutionary dynamics of climate-induced range shifts in sexually reproducing, diploid populations with both dispersal and environmental niche traits defined by multiple loci. In contrast, previous models have focused on a subset of these factors: ecological dynamics (e.g. (Brooker et al., 2007)), evolution in a single trait only (e.g. (Atkins and Travis, 2010; Henry et al., 2013)), and relatively simple genetic scenarios (e.g. single-locus haploid genetics in asexual populations (Boeye et al., 2013; Hargreaves et al., 2015)). Here, we tested the generality of previous ~~results~~ [predictions of an important role for dispersal evolution in range shifts \(Boeye et al., 2013; Henry et al., 2013\)](#) and

282 the interplay of eco-evolutionary dynamics under increased levels of biological complexity. Specifically, we demonstrated the role of spatial population structure, ~~in-driven by a gradient in the niche optimum and the starkness of the form of local adaptation and the environmental gradient defining~~
285 ~~the~~ range edge, in determining extinction risk for range shifting populations via impacts on the ~~initial equilibrium~~ distribution of dispersal phenotypes and environmental niche values.

Our results suggest that populations ~~most likely to keep pace with climate change will be~~
288 ~~those with little to no local adaptation within the pre-expansion, stable range and in locations with shallow environmental gradients defining the range edge characterized by local adaptation~~
~~to a spatially varying trait optimum and by stark range edges will be less able to track changing~~
291 ~~climatic conditions~~ (Fig. 2). A survey of the scientific literature found evidence for local adaptation in approximately 71% of studies, suggesting a high prevalence of local adaptation in natural populations (Hereford, 2009). ~~While it is difficult to exactly map the gradient in the niche optimum~~
294 ~~to empirical measures of local adaptation, the parameters defining the steepest gradient used here resulted in the intrinsic formation of stable range boundaries, as seen in previous theoretical studies (Alleaume-Benharira~~
~~suggesting they provide reasonable approximations of empirical patterns.~~ Further, a recent meta-
297 analysis of 1400 bird, mammal, fish, and tree species found no evidence for consistent declines in abundance towards range edges (Dallas et al., 2017), suggesting many species exhibit similar abundances at the edge and center of their ranges similar to the ~~stark environmental gradients~~ ~~starkest~~
300 ~~range edges~~ imposed in our study. While some of these patterns could represent a publication bias, for example against negative results in studies of local adaptation, combined with our results they suggest many species will face elevated extinction risks in climate-induced range shifts due to ~~the~~
303 ~~their~~ spatial population structure ~~of their initial ranges~~.

Our results emphasize the importance of the ~~initial equilibrium~~ distribution of dispersal phenotypes ~~composing the stable range (i.e. prior to the onset of rapid climate change)~~ in determin-

ing a population's extinction risk during climate change (Fig. 3c&d). ~~Survival in the face of~~
~~climate change was primarily determined by the dispersal phenotypes making up the population,~~
~~specifically whether the population included individuals with dispersal phenotypes at or above~~
~~a threshold value~~Populations primarily composed of high dispersal phenotypes at equilibrium
 successfully tracked changing climate conditions, while populations of lower dispersal phenotypes
 lagged behind the changing conditions to eventually go extinct. Importantly, the threshold necessary
~~to survive climate change itself~~ dividing the equilibrium dispersal phenotypes of successful and
~~extinct populations~~ was constant across all ~~parameter combinations~~ scenarios for a given speed
 of climate change (Fig. B9-B11). ~~Scenarios with no potential for local adaptation and gradual~~
~~environmental gradients had larger proportions of high dispersal phenotypes under stable climate~~
~~conditions, and therefore a lower probability of extinction during climate change. A high potential~~
~~for local adaptation, in contrast, selected against such high dispersal phenotypes due to dispersal's~~
~~homogenizing effect on population genetic structure (Lenormand, 2002)~~B9-11). Thus, the difference
 in survival probability among scenarios was driven by the effects of spatial population structure on
 the evolution of dispersal ability throughout the range. Scenarios with a steep gradient in the niche
 optimum selected for lower dispersal phenotypes at equilibrium due to the potential mismatch
 of dispersing individuals' niche phenotype and their new location (Kirkpatrick and Barton, 1997).
 Similarly, a ~~more severe habitat gradient at the range edge increased~~ stark range edge selected for
~~lower dispersal due to~~ the risk of dispersing ~~beyond the boundary of suitable habitat, resulting in~~
~~selection against heightened dispersal into unsuitable habitat~~ (Shaw et al., 2014). Thus, attributes
 defining the spatial structure of the range altered the distribution of dispersal phenotypes under
~~stable climate conditions, subsequently determining the extinction risk of populations during climate change~~Previous
 research has documented a similar reduction in dispersal phenotypes due to an explicit mortality
 cost of dispersal (Kubisch et al., 2013), whereas the costs to dispersal in our model arise intrinsically

330 ~~as a result of the spatial population structure. Such a cost to dispersal results in lower dispersal~~
~~phenotypes at equilibrium, hampering a population's ability to successfully track a changing climate.~~
Importantly, dispersal evolution during climate change was unable to counter the influence of initial
333 spatial population structure on extinction dynamics.

While high dispersal phenotypes ~~prior to climate change~~ at equilibrium increased the probability that populations tracked changing conditions, ~~it~~ they had the additional effect of reducing average fitness at the range edges when ~~populations had a moderate to high potential for local adaptation~~
336 ~~the niche optimum varied across the range~~ (Fig. B3-B5). In the model, ~~populations at the range~~
~~edges~~ range edge populations tended to have lower abundance than ~~populations in the range core~~
339 core populations, increasing their susceptibility to gene flow from the core (~~Lenormand, 2002~~) (García-Ramos and Kirkpatrick, 2002).
Thus, in populations with high dispersal phenotypes ~~prior to climate change~~ at equilibrium, increased gene flow from the core ~~likely~~ reduced fitness at the range edge ~~by preventing adaptation~~
342 ~~to local conditions~~ via gene swamping (Lenormand, 2002). As a result, the populations most likely to survive climate change were, counterintuitively, also those characterized by lower fitness at the range edges ~~prior to the onset of climate change~~ at equilibrium. While not all populations are characterized by small populations at the range edges (Dallas et al., 2017), our results suggest that
345 ~~populations exhibiting high levels of local adaptation within their stable range are likely to be at greater risk of extinction during periods of climate change~~ high fitness in edge populations may be
348 a warning sign of future difficulty in tracking climate change when the population is structured along a spatial gradient in a trait optimum. For the purposes of this investigation, we assumed the niche optima shifted spatially with climate change, as would be expected if the niche optima corresponded to local temperature or precipitation conditions (Davis and Shaw, 2001). However, in
351 systems characterized by a gradient in the niche optimum defined by other factors (e.g. geography or biotic interactions) the gradient might remain stable or even shift in an opposing direction to

354 climate change. Future research should investigate the impact of a gradient in the niche optimum
unrelated to climate on extinction risk during range shifts.

Previous research has suggested that evolution of increased dispersal ability during climate
357 change may be ~~a key mechanism in~~ capable of rescuing populations that would otherwise be unable
to keep pace with shifting environmental conditions (~~Boeye et al., 2013~~)(Boeye et al., 2013; Henry et al., 2013).

Our results suggest this is not always the case, and in fact may only be possible under certain,
360 relatively narrow conditions. Previous models showing that dispersal evolution may rescue popu-
lations during climate change have typically used relatively simple genetic frameworks to model
dispersal, including haploid genetics with a single-locus defining dispersal (Boeye et al., 2013;
363 Hargreaves et al., 2015). As dispersal evolution during range expansions and shifts occurs via the
spatial sorting of alleles contributing to heightened dispersal at the range edge (Shine et al., 2011),
such simplified genetic frameworks may allow more efficient sorting of such alleles compared
366 to situations with more complex genetic structure underlying the dispersal trait. ~~The negligible~~
~~role played by dispersal evolution in our model (Fig. 3a&b) suggests that when such simplifying~~
~~assumptions are relaxed, the potential for population rescue via evolution of heightened dispersal is~~
369 ~~greatly reduced, thus increasing the role of the initial spatial population structure within the range~~
~~in determining a population's fate under climate change~~ Additionally, the interaction of mutation
and genetic architecture in different models (e.g. few mutations of large effects or many mutations
372 of small effects) undoubtedly plays a role in dispersal evolution during range shifts. Increasing
mutation rate or effect size might have the equivalent effect of a slower speed of climate change
in allowing dispersal evolution to play a greater role in range shift dynamics. Further, life history
375 has been shown to impact the maintenance of genetic diversity, and hence evolutionary potential,
with stage and age-structured populations shown to harbor greater diversity than populations with
non-overlapping generations as modeled here (Ellner, 1996). Populations defined by more complex

378 life histories might, therefore, contain more genetic diversity in dispersal at equilibrium, making
evolution of increased dispersal during range shifts more likely. Thus, further research is needed to
understand how factors such as genetic architecture, mutational dynamics, and life history might
381 interact to shape the potential for population rescue via dispersal evolution during range shifts.

Conclusion

As climate change continues to threaten populations, communities, and ecosystems (Chen et al.,
384 2011; Gonzalez et al., 2010; Hobbs et al., 2009), it is increasingly important to understand pop-
ulation responses to changing environmental conditions. In particular, a deeper, process-based
understanding of extinction risk in populations undergoing range shifts will, in turn, allow more
387 focused conservation interventions. Our results suggest that ~~the initial~~ spatial population struc-
ture, as determined by ~~local adaptation and the environmental gradient at~~ gradients in the niche
optimum and the starkness of the range edge, has the potential to dramatically alter the extinction
390 ~~probability faced by~~ risk for species responding to climate change. Further, in contrast to other
studies assuming more simplified genetic structures, we find very little role for the evolution of
heightened dispersal abilities in allowing a population to successfully track climate change. Fu-
393 ture work should continue to examine the ~~interplay between initial conditions in range shifts and~~
~~circumstances determining~~ the potential for ~~evolutionary rescue~~ rescue via dispersal evolution in
range shifts. As climate change continues to accelerate (Chen et al., 2017), it is imperative to ~~not~~
396 ~~only~~ identify those factors leading to increased extinction risk in range shifting populations, ~~but~~
~~also and use that knowledge~~ to develop meaningful conservation strategies to mitigate such risk.

Appendix A: Full model description

Model overview

Purpose

This model ~~tests~~tested an evolving population's ability to track a changing climate under a variety
402 of conditions. Specifically, populations ~~are~~were simulated under different combinations of (1) the
~~starkness of the range boundary~~slope of a gradient in the niche optimum and (2) the ~~potential for~~
~~local adaptation~~starkness of the range edge. In all simulations, an individual's expected dispersal
405 distance and environmental niche ~~are~~were defined by an explicit set of quantitative diploid loci
subject to mutation, thus allowing both traits to evolve over time. All simulations ~~begin~~began
with stable climate conditions for 2000 generations to allow the populations to reach a spatial
408 equilibrium before the onset of climate change. Climate change ~~is~~was then modeled as a constant,
directional shift in ~~the location of environmentally suitable habitat~~environmental conditions (see
Submodels below). Finally, simulations ~~end~~ended with another short period of climate stability to
411 assess the population's ability to persist and recover after shifting its range.

State variables and scales

The model ~~simulates~~simulated a population of males and females characterized by diploid loci
414 for both their expected dispersal distance and environmental niche. Space ~~is~~was modeled as a
lattice of discrete patches overlaying a continuous Cartesian coordinate system. Landscapes ~~are~~
~~were~~ two dimensional with a fixed width along the y ~~axis~~dimension and without bounds on the x
417 ~~axis~~dimension. Environmental conditions ~~vary~~varied along the x dimension but ~~remain~~remained
constant within the y dimension. To avoid edge effects due to the fixed width of the y dimension,

the model ~~employs~~employed wrapping boundaries such that if an individual ~~disperses~~dispersed out of the landscape on one side, it ~~appears~~would appear at the opposite end of the same column of the landscape. Patches ~~are~~were defined by the location of the patch center in x and y coordinates and a patch width parameter defining the relationship between continuous Cartesian space and the discrete patches used for population dynamics (*Submodels*).

The model ~~implements~~implemented climate change by shifting the location of ~~a population's available habitat~~patch carrying capacities and the gradient in the niche optimum along the x dimension of the landscape. ~~Available habitat (i.e. a population's potential range) is defined by a center location on the~~ Patch carrying capacities were defined by the location of the range center along the x dimension, the ~~severity~~starkness of the decline ~~in habitat quality at the edge~~characterizing the range edges, and the width of the ~~available habitat~~range along the x dimension (See Figure A1). ~~Further, a gradient in environmental conditions is imposed throughout the landscape to allow for local adaptation via matching of an individual's environmental niche to the local environmental conditions (Submodels). The severity of this gradient can be altered to change the potential for local adaptation (e.g. a shallower gradient will result in more similar environmental conditions throughout the range and therefore reduce the potential for local adaptation)~~The gradient in the niche optimum was linear and shifted at the same speed and in the same direction as carrying capacities during climate change.

[Figure A1 goes here]

Process overview and scheduling

Time ~~is~~was modeled in discrete intervals defining single generations of the population (Fig. A2). Within each generation, individuals first ~~disperse~~dispersed from their natal patches according to their phenotypes. After dispersal, reproduction ~~occurs according to~~occurred via a stochastic im-

plementation of the classic Ricker model (Ricker, 1954) taking into account the mean fitness of individuals within the patch. Reproduction ~~occurs~~occurred via random sampling of the local population (with replacement) weighted by individual relative fitness such that individuals with high
444 relative fitness (as determined by the match between their environmental niche and local conditions) ~~are~~were likely to produce multiple offspring while individuals with low relative fitness ~~may~~
447 might not produce any. Individuals ~~inherit~~inherited one allele from each parent at each loci, assuming independent segregation and a mutation process. After reproduction, all individuals in the current generation ~~perish~~perished and the offspring ~~begin~~began the next generation with dispersal,
450 resulting in discrete, non-overlapping generations.

[Figure A2 goes here]

Design concepts

453 *Emergence*

Emergent phenomena in this model ~~include the spatial equilibrium of population abundances and trait values within the stable range, the demographic dynamics of the shifting population during~~
456 ~~climate change,~~included the spatial distribution of population abundance, dispersal abilities, and relative fitness throughout the range. (i.e. the spatial population structure). Additionally, the population dynamics during the range shift, including the extinction process, and the evolutionary
459 trajectories of ~~both expected dispersal distances and environmental niche values during climate change~~the dispersal and niche traits were all emergent phenomena in this model.

Stochasticity

462 All biological processes in this model ~~are~~were stochastic including realized population growth
in each patch, dispersal distances of each individual, and inheritance of loci. Environmental
parameters ~~are~~were fixed, however, and the process of climate change (i.e. the movement of
465 ~~environmentally-suitable-habitat~~patch carrying capacity through time) ~~is~~was deterministic. Thus,
the model ~~removes~~removed the confounding influence of environmental stochasticity to focus on
demographic and evolutionary dynamics of range shifts.

Interactions

468 Individuals in the model ~~interact~~interacted via mating and density-dependent competition within
patches. Additionally, the evolutionary trajectories of the two different traits ~~have~~had the potential
471 to interact via the relationship between gene flow (dispersal trait) and local adaptation (niche trait).
Further, ~~aspects determining the spatial population structure of a population's range (potential for~~
~~local adaptation and the nature~~the gradient in the niche optimum and the starkness of the range
474 edge ~~)can~~could interact with trait evolution within the range both during stable climate conditions
and during climate change.

Desired output

477 After each model run, full details of all surviving individuals at the last time point ~~are~~were recorded
(spatial coordinates and loci values for both traits). If a population went extinct during the model
run, the time of extinction ~~is~~was recorded. For each occupied patch throughout the simulation,
480 we aggregated data on population size, the dispersal trait, and ~~local adaptation to environmental~~
adaptation to local conditions.

Details

Initialization

483

The following parameters ~~are~~ were set at the beginning of each simulation and ~~form~~ formed the initial conditions of the model: the mean and variance for allele values of each trait, population
486 size, location of ~~environmentally-suitable-habitat~~ the range center, number of generations for the pre-, post-, and ~~during-rapid~~ climate change periods of the simulation, and all other necessary parameters for the submodels defined below. Simulated populations ~~are~~ were initialized in the
489 center of the range and allowed to spread and equilibrate throughout the range during the period of stable climate conditions. This ~~ensures~~ ensured that the populations reacting to a changing climate truly ~~represent~~ represented the expected spatial distribution for a given range, rather than the initial
492 parameter values used in the simulation ~~—See Tables (Table A1& A2 for a full list of parameter values used in the simulations described here).~~ Initial population size was chosen to minimize the risk of stochastic extinction in the early stages of the simulation. The time frames defining climate
495 change were designed to give a reasonable period for the population to reach a spatial equilibrium and a long enough period of climate change for extinction dynamics to play out. The number of patches defining the y dimension and the relationship between Cartesian space and discrete
498 patches were chosen to allow a reasonable number of patches to contribute to the eco-evolutionary dynamics of range shifts while not proving computationally restrictive.

Submodels

~~Environmentally-suitable-habitat~~ Patch carrying capacities. ~~Environmentally-suitable-habitat is determined by the population's carrying capacity as it ranges in space~~ Patch carrying capacity

Parameter	Description	Value
N_1	Initial population size (seeded across multiple patches) when beginning the simulations	2500 <u>individuals</u>
β_1	Center of environmentally-suitable-habitat <u>the range</u> before climate change	0
η—Spatial dimensions of—habitat patches—in continuous space—50 y_{max}—Number of—patches the—discrete lattice extends in—the—y direction—10 \hat{t}	Last time-point <u>generation</u> of stable climate conditions	2000
t_Δ	Duration of climate change	100 <u>generations</u>
t_{max}	Total number of time-points <u>generations</u> in the simulation	2150 <u>generations</u>
R—η	Intrinsic growth rate of the population <u>Width of square habitat patches in Cartesian space</u>	2–50
K_{max}—y_{max}	Maximum achievable carrying capacity in the range	0.5–10 patches

(K_x) ~~The carrying capacity is maximized in the center of the species' range (K_{max}) and declines with increasing~~ varied along the x dimension of the landscape, attaining its highest value at the range center and declining with distance from the center. Specifically, the carrying capacity at a location x ~~is~~ was defined as the product of the maximum potential carrying capacity (K_{max}) and a function $f(x, t)$, where $f(x, t)$ ~~ranges from~~ was bounded between 1 ~~in~~ and 0 with its highest value corresponding to the range center ~~to 0 far away from the center and is defined as follows~~. $f(x, t)$ was defined as

$$f(x, t) = \begin{cases} \frac{e^{\gamma(x-\beta_t+\tau)}}{1+e^{\gamma(x-\beta_t+\tau)}} & x \leq \beta_t \\ \frac{e^{-\gamma(x-\beta_t-\tau)}}{1+e^{-\gamma(x-\beta_t-\tau)}} & x > \beta_t \end{cases} \quad (A1)$$

where β_t ~~defines~~ defined the center of the ~~area of suitable habitat range~~ at time t , τ ~~sets~~ affected the width of the range, and γ ~~affects~~ affected the slope of the function at the range ~~boundaries edges~~ (See Figure A1). ~~To understand the relationship between γ and the slope of $f(x, t)$ at the range boundary, the partial derivative of $f(x, t)$ over the x dimension can be shown to be~~

$$f(x, t) = \begin{cases} \frac{\gamma e^{\gamma(x-\beta_t+\tau)}}{(1+e^{\gamma(x-\beta_t+\tau)})^2} & x \leq \beta_t \\ \frac{-\gamma e^{-\gamma(x-\beta_t-\tau)}}{(1+e^{-\gamma(x-\beta_t-\tau)})^2} & x > \beta_t \end{cases}$$

501 yielding a value of $\pm \frac{\gamma}{4}$ at the inflection points on either side of the range center ($x = \beta_t \pm \tau$).

~~Population dynamics occur~~ Population dynamics occurred within discrete patches, so to calculate a K_x value for a discrete patch from the continuous function $f(x, t)$, we ~~use~~ used another parameter defining the spatial scale of each patch (η ; ~~See Figure A1~~). The local carrying capacity of a patch centered on x (K_x) ~~is~~ was then calculated as the mean of $f(x, t)$ over the interval of the patch multiplied by K_{max} .

$$K_x = \frac{K_{max}}{\eta} \int_{x-\frac{\eta}{2}}^{x+\frac{\eta}{2}} f(x, t) dx \quad (A2)$$

By varying the parameters defining $f(x, t)$, we can change both the total carrying capacity of the population, summed across all patches throughout the range, (by altering both τ and β_t) and the slope at which K_x declines to 0 (by altering of $f(x, t)$ at the range edge, we calculated the partial derivative of $f(x, t)$ over the x dimension as

$$\frac{\partial f(x, t)}{\partial x} = \begin{cases} \frac{\gamma e^{\gamma(x - \beta_t + \tau)}}{(1 + e^{\gamma(x - \beta_t + \tau)})^2} & x \leq \beta_t \\ \frac{-\gamma e^{-\gamma(x - \beta_t - \tau)}}{(1 + e^{-\gamma(x - \beta_t - \tau)})^2} & x > \beta_t \end{cases} \quad (\text{A3})$$

yielding a value of $\pm \frac{\gamma}{4}$ at the inflection points on either side of the range center ($x = \beta_t \pm \tau$). Thus, altering γ . Changing the slope affects not only the rate at which K_x declines at the range boundaries (our focus), but it also alters the total carrying capacity of the population. To avoid this confounding factor, we fix directly altered the starkness of the range edge. However, changing γ also changed the total area under the curve $f(x, t)$. The as can be seen in the indefinite integral of $f(x, t)$ can be shown to be:

$$\int_{-\infty}^{\infty} f(x, t) dx = \frac{2 \ln(e^{\gamma \tau} + 1)}{\gamma} \quad (\text{A4})$$

which can be solved for τ . For a given fixed total area under the curve, an appropriate value of τ can be calculated for each value of γ . Thus, ranges defined by different γ .

Thus, values could also result in different range-wide carrying capacities, potentially altering both the ecological (e.g. through stochastic extinction events) and evolutionary (e.g. through the efficiency of selection relative to drift) dynamics of the ranges. Additionally, different combinations of γ and τ are both fixed within a given simulation and β_t (the location of the center of suitable habitat) is used to simulate climate change. During the periods before and after climate change β_t is constant, but to simulate climate change it varies with time as follows:

$$\beta_t = v\eta(t - \hat{t})$$

504 where v is the velocity of climate change per generation in terms of discrete patches, t is the
current generation, and \hat{t} is the last generation of stable climatic conditions before the onset of
climate change. could result in different range widths, which have been shown to impact dispersal
507 evolution within the ranges (Van Kirk and Lewis, 1997). To control for these confounding factors,
we fixed the range widths for all scenarios and altered K_{max} to maintain a constant range-wide
carrying capacity. Specifically, we defined the range width using the x coordinates at which $f(x, t)$
510 fell below 0.1 on either side of β_t and chose τ and γ values for each scenario such that $f(x, t)$ fell
below 0.1 at the same x coordinates (Table A2). We then adjusted K_{max} for each scenario so that
the range-wide carrying capacity was constant (Fig. A3).

513 [Figure A3 goes here]

Local adaptation. To allow an arbitrary degree of local adaptation within the range, the local
environmental optima for each patch ($z_{opt,x}$) are set as follows. Thus, γ and τ were both fixed within
a given simulation and β_t (the location of the range center) was used to simulate climate change.
During the periods before and after climate change β_t was constant, but to simulate climate change
it varied with time as follows

$$z_{opt,x} = \lambda(x - \beta_t = v\eta(t - \hat{t})) \quad (A5)$$

where v was the velocity of climate change per generation in terms of discrete patches, t was the
current generation, and \hat{t} was the last generation of stable climatic conditions before the onset of
516 climate change.

Environmental niche. The niche optimum ($z_{opt,x}$) varied in space according to

$$z_{opt,x} = \lambda(x - \beta_t) \quad (A6)$$

with λ defines the potential for local adaptation with values close to 0 resulting in little to no

Habitat gradient at the <u>Starkness of range edge</u>	Potential for local adaptation <u>Slope of niche</u> <u>optimum</u>	γ	τ	λ	K_{max}
Shallow	None <u>Flat</u>	0.0025	250 <u>-240</u>	0	<u>240</u>
	Low <u>Shallow</u>	0.0025	250 <u>-240</u>	0.004	<u>240</u>
	High <u>Steep</u>	0.0025	250 <u>-240</u>	0.008	<u>240</u>
Moderate	None <u>Flat</u>	0.025 <u>0.0075</u>	421.479 <u>345.9</u>	0	<u>118.1</u>
	Low <u>Shallow</u>	0.025 <u>0.0075</u>	421.479 <u>345.9</u>	0.004	<u>118.1</u>
	High <u>Steep</u>	0.025 <u>0.0075</u>	421.479 <u>345.9</u>	0.008	<u>118.1</u>
Stark	None <u>Flat</u>	0.25	421.48 <u>630.1</u>	0	<u>66.7</u>
	Low <u>Shallow</u> 28	0.25	421.48 <u>630.1</u>	0.004	<u>66.7</u>
	High <u>Steep</u>	0.25	421.48 <u>630.1</u>	0.008	<u>66.7</u>

Table A2: Descriptions and parameter values for the 9 different experimental scenarios. [As defined](#)

change in environmental optima across the range and values of greater magnitude resulting in large differences in environmental optima determining the rate of change in the optimum across the range. Individual relative fitness ($w_{i,x}$) values ~~are~~ were then calculated according to the following equation assuming stabilizing selection

$$w_{i,x} = e^{\frac{-(z_i - z_{opt,x})^2}{2\omega^2}} \quad (A7)$$

where ω ~~defines~~ defined the strength of stabilizing selection and z_i ~~is~~ was an individual's niche phenotype (Lande, 1976). Thus, an individual's realized fitness ~~will be~~ was higher the closer its
 519 niche phenotype (z_i) ~~is~~ was to the environmental optimum of the patch it ~~occupies~~ occupied ($z_{opt,x}$). All loci ~~are~~ were assumed to contribute additively to an individual's environmental niche value with no dominance or epistasis, meaning an individual's phenotype ~~is~~ was simply the sum of the
 522 individual's allele values. As defined above, $z_{opt,x}$ also shifts with climate change (i.e. with β_t) as would be expected if it corresponded to a phenotypic optimum along a temperature or precipitation gradient within the range (Davis and Shaw, 2001).

Population dynamics. Population growth within each patch ~~is~~ was modeled with a stochastic implementation of the classic Ricker model (Melbourne and Hastings, 2008; Ricker, 1954). To account for fitness effects on population growth, expected population growth ~~is~~ was scaled by the mean relative fitness of individuals within the patch (\bar{w}_x) so that maladaptation resulted in reduced population growth. The expected number of new offspring in patch x at time $t + 1$ ~~is then~~ was given by

$$\hat{N}_{t+1,x} = \bar{w}_x F_{t,x} \frac{R}{\psi} e^{\frac{-RN_{t,x}}{K_x}} \quad (A8)$$

where $F_{t,x}$ ~~is~~ was the number of females in patch x at time t , R ~~is~~ was the intrinsic growth rate for the population and remained constant in both time and space, ψ ~~is~~ was the expected sex ratio of the population, $N_{t,x}$ ~~is~~ was the number of individuals (males and females) in patch x at time t ,

and K_x ~~is~~-was the local carrying capacity based on the environmental conditions. To incorporate demographic stochasticity, the realized number of offspring for each patch ~~is~~-was then drawn from a Poisson distribution.

$$N_{t+1,x} \sim \text{Poisson}(\hat{N}_{t+1,x}) \quad (\text{A9})$$

525 Parentage of the offspring ~~is-then~~-was assigned by random sampling of the local male and female ~~population~~-populations (i.e. polygynandrous mating assuming a well-mixed population within each patch). The sampling ~~is~~-was weighted by individual fitness and ~~oeurs~~-occurred with
528 replacement so highly fit individuals ~~are~~-were likely to have multiple offspring while low fitness individuals ~~may-not-have~~-might not have had any. Each offspring ~~inherits~~-inherited one allele per locus from each parent, assuming no linkage among loci. After reproduction, all members of the
531 previous generation ~~die~~-died and the offspring ~~disperse~~-dispersed to begin the next generation. Parameters governing population dynamics (Table A3) were chosen to yield reasonable rates of population growth based on initial exploratory simulations.

Mutation. Inherited alleles ~~are~~-were subject to mutation such that some offspring might not inherit identical copies of certain alleles from their parents. The mutation process ~~is~~-was defined by two parameters for each trait T : the diploid mutation rate (U^T) and the mutational variance (V_m^T). Using these parameters along with the number of loci defining trait T (L^T), the per locus probability of a mutation ~~is~~-was

$$\frac{U^T}{2L^T} \quad (\text{A10})$$

~~Mutational effects are~~-Effect sizes of mutations were drawn from a normal distribution with mean 0 and a standard deviation of

$$\sqrt{V_m^T U^T} \quad (\text{A11})$$

<u>Parameter</u>	<u>Description</u>	<u>Value</u>
<u>R</u>	<u>Intrinsic growth rate of the population</u>	<u>2</u>
<u>ψ</u>	<u>Expected sex ratio (females/males) in the population</u>	<u>0.5</u>
<u>\hat{d}</u>	<u>Maximum achievable dispersal phenotype</u>	<u>1000</u>
<u>ρ</u>	<u>Determines the slope of the transition in dispersal phenotypes from 0 to D</u>	<u>0.5</u>

Table A3: Values and descriptions for parameters related to population growth and dispersal.

534 ~~By meaning the ratio of small effect versus large effect mutations depended on both U^T and V_m^T . We chose parameter values (Table A4) in keeping with previously derived values from the literature (Gilbert et al., 2017). For the number of loci used in our simulations, these resulted in~~
537 ~~mostly mutations of small effect with few large effect mutations. Importantly, by defining the mu-~~
~~tation process in this manner rather than setting a way, rather than with a per locus probability of~~
~~mutation and mutational effect directly, similar mutational dynamics can be imposed a mutation~~
540 ~~effect size directly, the mutational input per generation was kept constant regardless of the number~~
~~of loci used in the simulation defining the trait (Schiffers et al., 2014).~~

Dispersal. Finally, individuals ~~disperse~~ dispersed according to an exponential dispersal kernel defined by each individual's dispersal phenotype. An individual's dispersal phenotype ~~is~~ was the expected dispersal distance and ~~is~~ was given by

$$d_i = \frac{\hat{d}\eta e^{\rho \Sigma L^D}}{1 + e^{\rho \Sigma L^D}} \quad (\text{A12})$$

where \hat{d} ~~is~~ was the maximum expected dispersal distance in terms of discrete patches, ρ ~~is~~ was a constant determining the slope of the transition between 0 and \hat{d} , and the summation ~~is~~ was taken across all alleles contributing to dispersal. Thus, as with fitness, loci ~~are~~ were assumed to contribute additively with no dominance or epistasis. The expected dispersal distance, d_i ~~is~~ was then used to draw a realized distance from an exponential dispersal kernel. ~~Since the dispersal phenotype is the expected value of the exponential dispersal kernel, it can be used directly to calculate the two dimensional diffusion coefficient of population spread (D). Specifically, since d_i^2 represents the mean squared displacement of an individual with dispersal phenotype d_i , the two dimensional diffusion coefficient can be calculated as~~

$$D = \frac{1}{4} d_i^2$$

<u>Parameter</u>	<u>Description</u>	<u>Value</u>
ω	Defines the strength of stabilizing selection on fitness traits	3
U^T	Diploid mutation rate for each trait	0.02
V_m^T	Mutational variance for each trait	0.0004
L^T	Number of diploid loci defining each trait	5 loci
μ_v^f	Initial mean allele value for the environmental niche trait	0
μ_v^d	Initial mean allele value for the dispersal trait	-1
σ_v^f	Initial standard deviation of allele values for the environmental niche trait	0.025
σ_v^d	Initial standard deviation of allele values for the dispersal trait	1

Table A4: Values and descriptions for parameters defining the genetic components of the model.

Once the realized dispersal distance is obtained, the direction of dispersal is ~~The direction of~~
 543 ~~dispersal (in radians) was~~ drawn from a uniform distribution bounded by 0 and 2π . If a dispersal
 trajectory ~~takes-took~~ an individual outside the bounds of the landscape in the y dimension, the
 individual ~~reappears-reappeared~~ at the same x coordinate but the opposite end of the y dimension,
 546 thus wrapping the top and bottom edges of the landscape to avoid edge effects. Dispersal ~~occurs~~
~~occurred~~ from the center of each patch and the individual's new patch ~~is-was~~ then determined
 according to its location in the overlaid grid of $\eta \times \eta$ patches (see Figure A1). ~~Dispersal parameters~~
 549 ~~(Table A3) were chosen to allow a wide range of dispersal phenotypes to evolve in the context of~~
~~the different experimental scenarios, ranging from highly restrictive to long-distance dispersal.~~

~~Since the dispersal phenotype was the expected value of the exponential dispersal kernel, it~~
~~could be used directly to calculate the two dimensional diffusion coefficient of population spread~~
~~(D). Specifically, since d_i^2 represented the mean squared displacement of an individual with~~
~~dispersal phenotype d_i , the two dimensional diffusion coefficient could be calculated as~~

$$D = \frac{1}{4} d_i^2 \quad (A13)$$

~~and subsequently used to calculate the approximate speed of an expansion wave defined by that~~
 552 ~~dispersal phenotype.~~

Appendix B: Supplementary results for varying speeds of climate change

Extinction probability

As in the main text, we calculated the cumulative probability of extinction for both slow and fast speeds of climate change here. The figures in this section use the same layout and line types as Figure 2 in the main text to allow for direct comparisons.

[Figures B1&B2 go here.]

~~Initial~~ Equilibrium fitness throughout the landscape

To assess trends in realized fitness values throughout the landscape, we calculated ~~the~~ patch-level mean individual fitness ~~value~~ for each landscape ~~just prior to the onset of climate change~~ at equilibrium. To simplify the figures, we averaged over the y dimension in which ~~environmental conditions do not vary. By separating the results for both extinction populations and those~~ CV in niche genotypes was minimal throughout the range for all scenarios (typically below 0.25) due to the constant environmental conditions. Populations at the range edge were characterized by reduced fitness compared to core populations, as found in previous models (García-Ramos and Kirkpatrick, 1997). However, this trend was exacerbated in populations that successfully tracked climate change ~~we identified a trend in which the edge populations displayed lower fitness in populations that were ultimately successful, particularly in simulations with a gradual environmental gradient at the range edge and compared to those that went extinct, especially in the~~ potential for local adaptation presence of gradual range edges and steep gradients in the niche optimum. As realized fitness values do not vary spatially in simulations with no ~~potential for local adaptation~~ gradient in the niche optimum,

the following figures only show results for scenarios with a ~~moderate or high potential for local~~
~~adaptation~~shallow or steep gradient.

576 [Figures B3-B5 go here.]

Dispersal evolution

Using the same metric of dispersal evolution from the main text (~~average change in~~ change in
579 average phenotype for each patch), we display here the observed dispersal evolution over the course
of climate change for all experimental scenarios. Each histogram in the following figures represents
a single experimental scenario as indicated by the figure text. The lower left panel and upper right
582 panel from Figure B7 are the same histograms shown in Figure 3a&b, but are here placed in the
context of all other experimental scenarios.

[Figures B6-B8 go here.]

585 ~~Initial~~ Equilibrium dispersal phenotypes

Here, we present histograms of the ~~initial~~ equilibrium distribution of dispersal phenotypes to
demonstrate the importance of those phenotypes in determining population success or extinction
588 during climate change. Dispersal phenotypes are log transformed for easier comparison. As with
the dispersal evolution section, each histogram represents a single experimental scenario as indi-
cated by the figure text. Similarly, the lower left panel and upper right panel from Figure B10 are
591 the same histograms shown in Figure 3c&d, but are here placed in the context of all other exper-
imental scenarios. All histograms additionally have a vertical dashed line indicating the dispersal
phenotype necessary to produce an expansion wave traveling at exactly the speed of climate change
594 in each simulation. This value serves as a threshold to distinguish individuals from ultimately suc-

cessful versus extinct populations.

[Figures B9-B11 go here.]

Literature Cited

597

- Aguilée, R., G. Raoul, F. Rousset, and O. Ronce. 2016. Pollen dispersal slows geographical range shift and accelerates ecological niche shift under climate change. *Proceedings of the National Academy of Sciences* 113:E5741–E5748.
- 600
- Alleaume-Benharira, M., I. Pen, and O. Ronce. 2006. Geographical patterns of adaptation within a species? range: interactions between drift and gene flow. *Journal of evolutionary biology* 19:203–215.
- 603
- Atkins, K., and J. Travis. 2010. Local adaptation and the evolution of species' ranges under climate change. *Journal of Theoretical Biology* 266:449–457.
- 606
- Bocedi, G., S. C. Palmer, G. Pe'er, R. K. Heikkinen, Y. G. Matsinos, K. Watts, and J. M. Travis. 2014. Rangesifter: a platform for modelling spatial eco-evolutionary dynamics and species' responses to environmental changes. *Methods in Ecology and Evolution* 5:388–396.
- 609
- Boeye, J., J. M. Travis, R. Stoks, and D. Bonte. 2013. More rapid climate change promotes evolutionary rescue through selection for increased dispersal distance. *Evolutionary Applications* 6:353–364.
- 612
- Brooker, R. W., J. M. Travis, E. J. Clark, and C. Dytham. 2007. Modelling species' range shifts in a changing climate: the impacts of biotic interactions, dispersal distance and the rate of climate change. *Journal of Theoretical Biology* 245:59–65.
- 615
- Case, T. J., and M. L. Taper. 2000. Interspecific competition, environmental gradients, gene flow, and the coevolution of species' borders. *The American Naturalist* 155:583–605.

- Chen, I.-C., J. K. Hill, R. Ohlemüller, D. B. Roy, and C. D. Thomas. 2011. Rapid range shifts of
618 species associated with high levels of climate warming. *Science* 333:1024–1026.
- Chen, X., X. Zhang, J. A. Church, C. S. Watson, M. A. King, D. Monselesan, B. Legresy, and
C. Harig. 2017. The increasing rate of global mean sea-level rise during 1993–2014. *Nature*
621 *Climate Change* 7:492.
- Dallas, T., R. R. Decker, and A. Hastings. 2017. Species are not most abundant in the centre of
their geographic range or climatic niche. *Ecology Letters* 20:1526–1533.
- 624 Davis, M. B., and R. G. Shaw. 2001. Range shifts and adaptive responses to quaternary climate
change. *Science* 292:673–679.
- Ellner, S. 1996. Environmental fluctuations and the maintenance of genetic diversity in age or
627 stage-structured populations. *Bulletin of Mathematical Biology* 58:103–127.
- Excoffier, L., M. Foll, and R. J. Petit. 2009. Genetic consequences of range expansions. *Annual*
Review of Ecology, Evolution, and Systematics 40:481–501.
- 630 Fisher, R. A. 1937. The wave of advance of advantageous genes. *Annals of eugenics* 7:355–369.
- García-Ramos, G., and M. Kirkpatrick. 1997. Genetic models of adaptation and gene flow in
peripheral populations. *Evolution* 51:21–28.
- 633 Gilbert, K. J., N. P. Sharp, A. L. Angert, G. L. Conte, J. A. Draghi, F. Guillaume, A. L. Harg-
reaves, R. Matthey-Doret, and M. C. Whitlock. 2017. Local adaptation interacts with expansion
load during range expansion: Maladaptation reduces expansion load. *The American Naturalist*
636 189:368–380.

- Gonzalez, P., R. P. Neilson, J. M. Lenihan, and R. J. Drapek. 2010. Global patterns in the vulnerability of ecosystems to vegetation shifts due to climate change. *Global Ecology and Biogeography* 19:755–768.
- Grimm, V., U. Berger, D. L. DeAngelis, J. G. Polhill, J. Giske, and S. F. Railsback. 2010. The odd protocol: a review and first update. *Ecological Modelling* 221:2760–2768.
- Hargreaves, A., S. Bailey, and R. A. Laird. 2015. Fitness declines towards range limits and local adaptation to climate affect dispersal evolution during climate-induced range shifts. *Journal of Evolutionary Biology* 28:1489–1501.
- Hargreaves, A. L., and C. G. Eckert. 2014. Evolution of dispersal and mating systems along geographic gradients: implications for shifting ranges. *Functional Ecology* 28:5–21.
- Hastings, A., K. Cuddington, K. F. Davies, C. J. Dugaw, S. Elmendorf, A. Freestone, S. Harrison, M. Holland, J. Lambrinos, U. Malvadkar, et al. 2005. The spatial spread of invasions: new developments in theory and evidence. *Ecology Letters* 8:91–101.
- Henry, R. C., G. Bocedi, and J. M. Travis. 2013. Eco-evolutionary dynamics of range shifts: elastic margins and critical thresholds. *Journal of Theoretical Biology* 321:1–7.
- Hereford, J. 2009. A quantitative survey of local adaptation and fitness trade-offs. *The American Naturalist* 173:579–588.
- Hobbs, R. J., E. Higgs, and J. A. Harris. 2009. Novel ecosystems: implications for conservation and restoration. *Trends in Ecology & Evolution* 24:599–605.
- Holt, R. D., T. H. Keitt, M. A. Lewis, B. A. Maurer, and M. L. Taper. 2005. Theoretical models of species' borders: single species approaches. *Oikos* 108:18–27.

- Kirkpatrick, M., and N. H. Barton. 1997. Evolution of a species' range. *The American Naturalist* 150:1–23.
- 660 Kubisch, A., T. Degen, T. Hovestadt, and H. J. Poethke. 2013. Predicting range shifts under global change: the balance between local adaptation and dispersal. *Ecography* 36:873–882.
- Lande, R. 1976. Natural selection and random genetic drift in phenotypic evolution. *Evolution* 30:314–334.
- 663 30:314–334.
- Lenormand, T. 2002. Gene flow and the limits to natural selection. *Trends in Ecology & Evolution* 17:183–189.
- 666 Loarie, S. R., P. B. Duffy, H. Hamilton, G. P. Asner, C. B. Field, and D. D. Ackerly. 2009. The velocity of climate change. *Nature* 462:1052.
- Melbourne, B. A., and A. Hastings. 2008. Extinction risk depends strongly on factors contributing to stochasticity. *Nature* 454:100.
- 669 to stochasticity. *Nature* 454:100.
- Mustin, K., T. G. Benton, C. Dytham, and J. M. Travis. 2009. The dynamics of climate-induced range shifting; perspectives from simulation modelling. *Oikos* 118:131–137.
- 672 Ochocki, B. M., and T. E. Miller. 2017. Rapid evolution of dispersal ability makes biological invasions faster and more variable. *Nature Communications* 8:14315.
- Parmesan, C. 2006. Ecological and evolutionary responses to recent climate change. *Annual Review of Ecology, Evolution, and Systematics* 37:637–669.
- 675 Review of Ecology, Evolution, and Systematics 37:637–669.
- Phillips, B. L. 2015. Evolutionary processes make invasion speed difficult to predict. *Biological Invasions* 17:1949–1960.

- 678 Polechova, J. 2018. Is the sky the limit? on the expansion threshold of a species? range. *PLoS*
biology 16:e2005372.
- Polechová, J., and N. H. Barton. 2015. Limits to adaptation along environmental gradients. *Pro-*
681 ceedings of the National Academy of Sciences page 201421515.
- Ricker, W. E. 1954. Stock and recruitment. *Journal of the Fisheries Board of Canada* 11:559–623.
- Schiffers, K., F. M. Schurr, J. M. Travis, A. Duputié, V. M. Eckhart, S. Lavergne, G. McNerny,
684 K. A. Moore, P. B. Pearman, W. Thuiller, et al. 2014. Landscape structure and genetic architec-
ture jointly impact rates of niche evolution. *Ecography* 37:1218–1229.
- Sexton, J. P., P. J. McIntyre, A. L. Angert, and K. J. Rice. 2009. Evolution and ecology of species
687 range limits. *Annu. Rev. Ecol. Evol. Syst.* 40:415–436.
- Shaw, A. K., M. Jalasvuori, and H. Kokko. 2014. Population-level consequences of risky dispersal.
Oikos 123:1003–1013.
- 690 Shaw, A. K., and H. Kokko. 2015. Dispersal evolution in the presence of allee effects can speed up
or slow down invasions. *The American Naturalist* 185:631–639.
- Shine, R., G. P. Brown, and B. L. Phillips. 2011. An evolutionary process that assembles pheno-
693 types through space rather than through time. *Proceedings of the National Academy of Sciences*
108:5708–5711.
- Szűcs, M., M. Vahsen, B. Melbourne, C. Hoover, C. Weiss-Lehman, and R. Hufbauer. 2017. Rapid
696 adaptive evolution in novel environments acts as an architect of population range expansion.
Proceedings of the National Academy of Sciences 114:13501–13506.

Team, R. C. 2000. R language definition. Vienna, Austria: R Foundation for Statistical Computing.

699

Van Kirk, R. W., and M. A. Lewis. 1997. Integrodifference models for persistence in fragmented habitats. *Bulletin of Mathematical Biology* 59:107.

702

Wallace, B. 1975. Hard and soft selection revisited. *Evolution* 29:465–473.

Weiss-Lehman, C., R. A. Hufbauer, and B. A. Melbourne. 2017. Rapid trait evolution drives increased speed and variance in experimental range expansions. *Nature Communications* 8:14303.

Figures

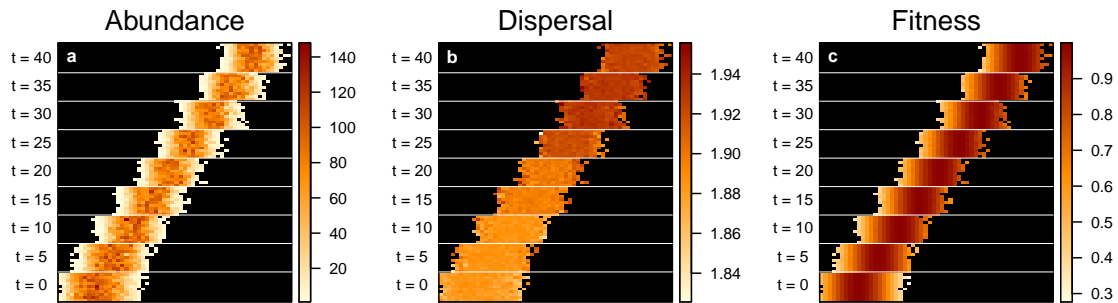


Figure 1: A single example of a simulation with a ~~high potential for local adaptation~~ steep gradient in the niche optimum and a moderate ~~habitat gradient defining the range edge~~. Information on the (a) abundance, (b) dispersal, and (c) fitness of individuals in each patch is shown for time periods beginning with the last generation of stable climate conditions ($t = 0$) to 40 generations after the start of climate change. Log transformed mean dispersal phenotypes (b) are shown for each patch. Average patch fitness (c) was calculated based on the mean ~~environmental~~ niche trait of local individuals and the ~~environmental~~ niche optima for each patch.

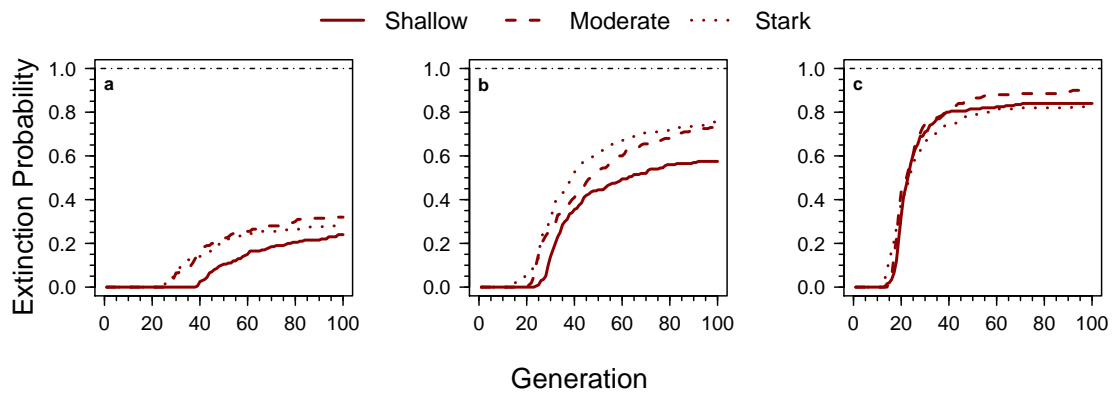


Figure 2: The cumulative probability of extinction due to a moderate speed of climate change in different experimental scenarios. Graphs show the proportion of simulated populations that went extinct through time for scenarios with a (a) no flat, (b) low shallow, and (c) high potential for local adaptation steep gradient in the niche optimum, and in environments ranges characterized by a shallow (solid line), moderate (dashed line), or stark (dotted line) gradient at the range edge edges.

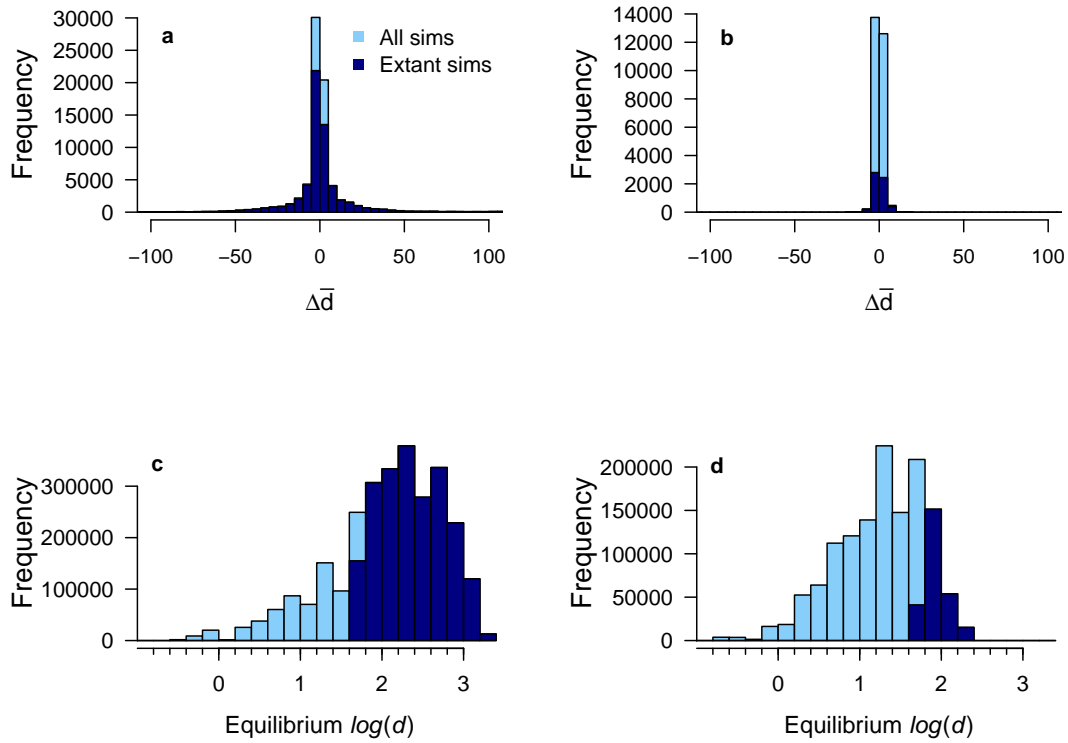


Figure 3: Patterns in the evolution and the initial distribution of the dispersal trait, highlighting extant simulations from a moderate speed of climate change. Evolution in dispersal (a and b) is shown as the change in the mean dispersal phenotype of each patch from the beginning of the period of climate change to the end. Positive values indicate an increase in average dispersal ability in the patch. Initial Equilibrium distributions of the dispersal trait (c and d) are shown as log transformed dispersal phenotypes of individuals in populations after 2000 generations of stable climate conditions. In all panels, values associated with extant populations are shown in dark blue. Results are shown for populations with no potential for local adaptation gradient in the niche optimum and a gradual environmental gradient at the range boundary edge (a and c; $n = 155$ extant populations) and for populations with a high potential for local adaptation steep gradient in the niche optimum and a stark gradient at the range boundary edge (b and d; $n = 14$ extant populations). Full results for all parameter combinations are provided in Appendix B.

Online figures

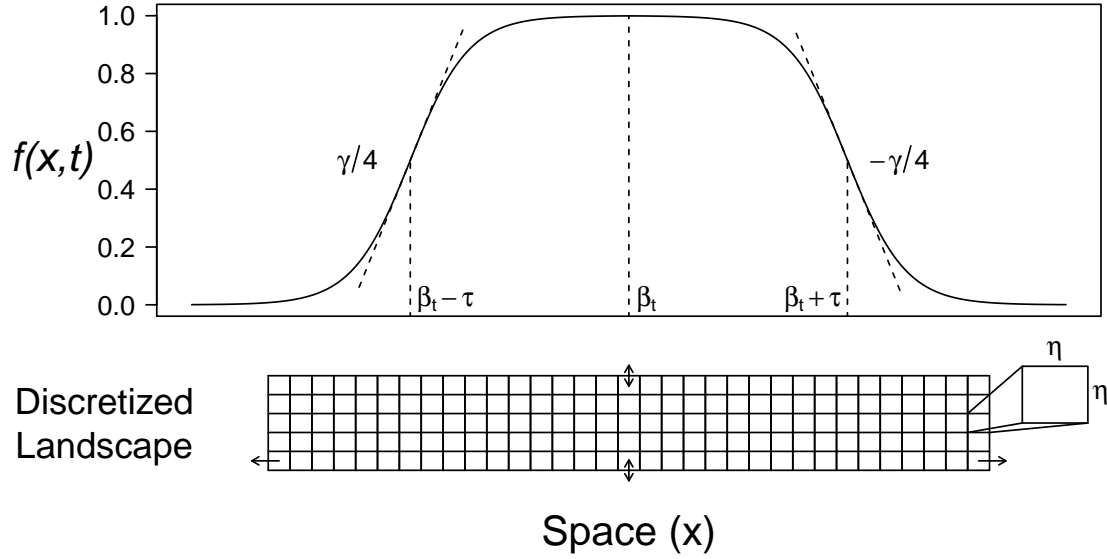


Figure A1: Example visualization of ~~the environmentally suitable habitat available to a population,~~ ~~as defined by~~ $f(x, t)$ in Cartesian space. The parameters of $f(x, t)$ are shown on the figure at significant points along the x axis. Specifically, β_t defined the center of the range, γ determined the slope of $f(x, t)$ at the inflection points (i.e. the range edges), and τ determined the location of the inflection points. The lattice of discrete $\eta \times \eta$ patches in which population dynamics ~~occur~~ occurred is shown beneath. As described in the *Submodels* section of the supplemental materials, $f(x, t)$ ~~determines~~ determined the carrying capacity of the ~~discrete $\eta \times \eta$ patches~~ . Carrying capacities vary with $f(x, t)$ along the x dimension of the lattice and remain while carrying capacity remained constant within each column along the y dimension. Landscapes ~~are~~ were unbounded in the x dimension and implemented with wrapping boundaries in the y dimension.

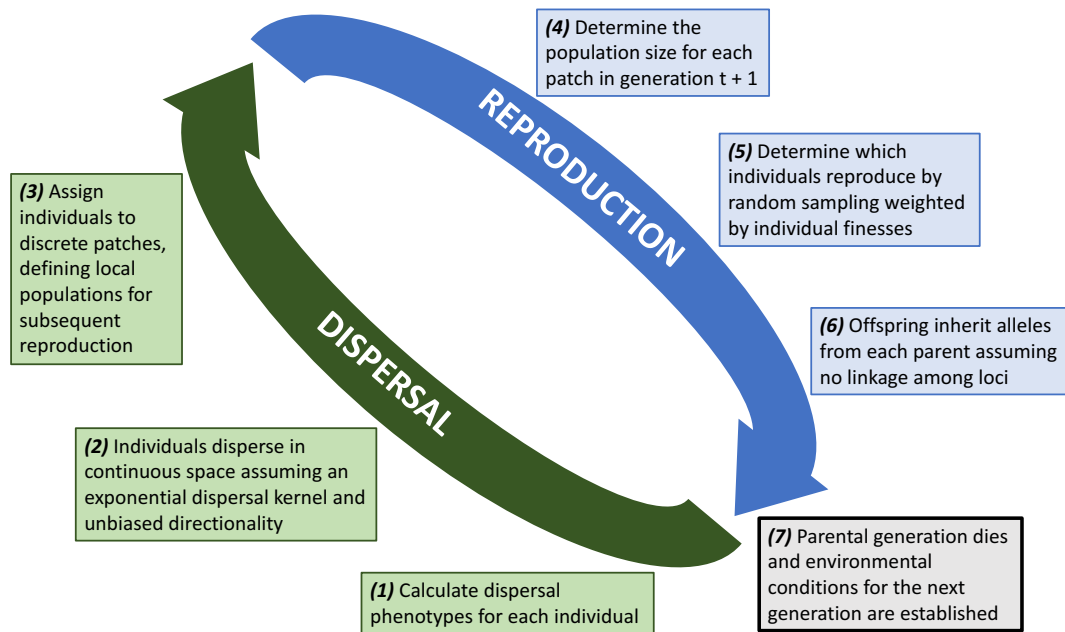


Figure A2: The life cycle of simulated populations is shown divided between events contributing to reproduction and dispersal. Each generation ~~begins~~began with new offspring dispersing according to their phenotype, after which reproduction ~~occurs~~occurred in local populations defined by the discrete lattice. After reproduction, all parental individuals ~~perish~~perished, resulting in discrete, non-overlapping generations.

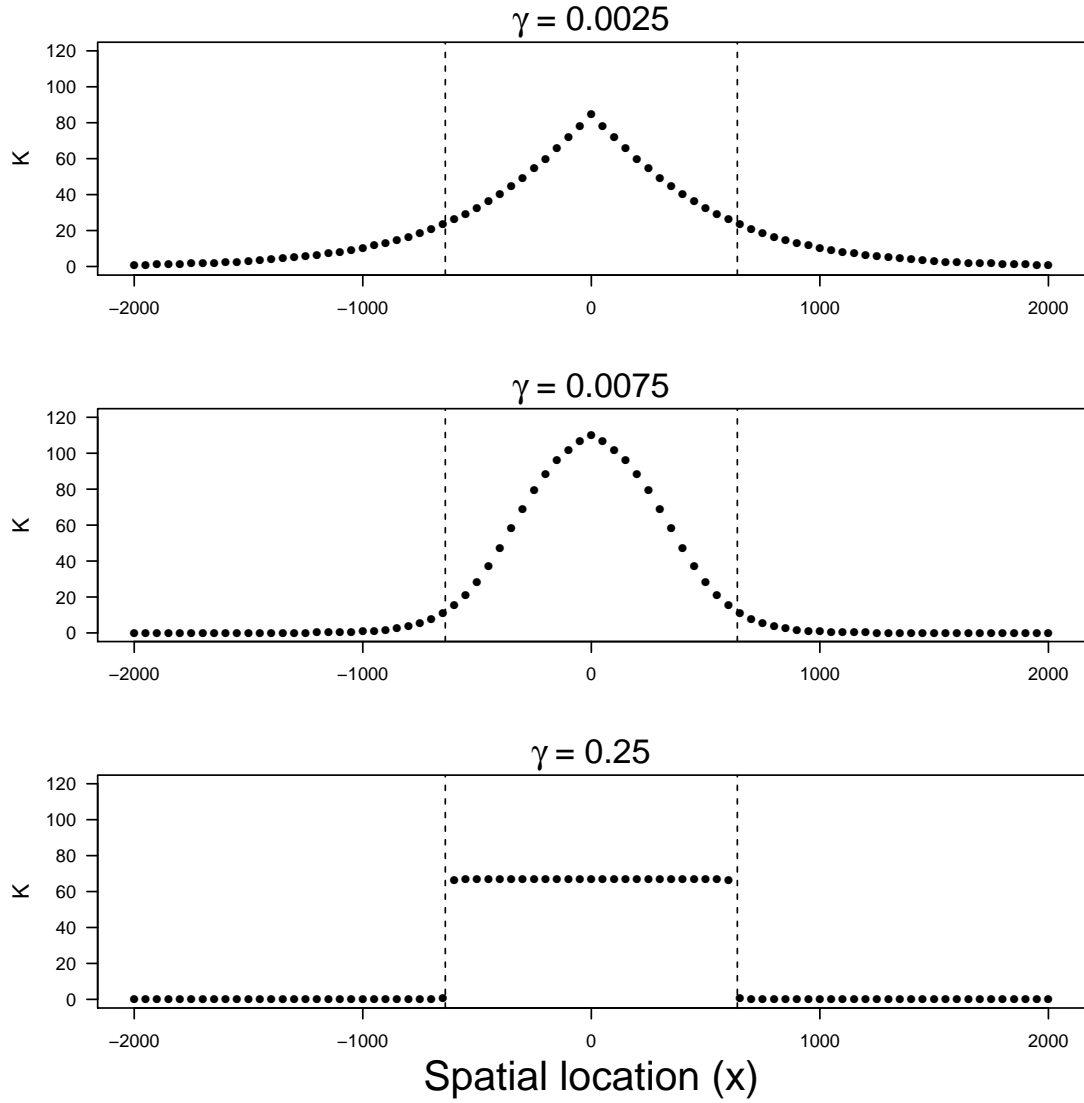


Figure A3: [The carrying capacity of discrete patches along the \$x\$ dimension of landscapes. From top to bottom, the plots show the carrying capacities for gradual, moderate, and stark range edges. Points represent the carrying capacity of a discrete \$\eta \times \eta\$ patch in the range. The vertical dashed lines indicate the \$x\$ coordinates at which \$f\(x, t\)\$ declines below 0.1 and the \$\gamma\$ value for each plot is listed above.](#)

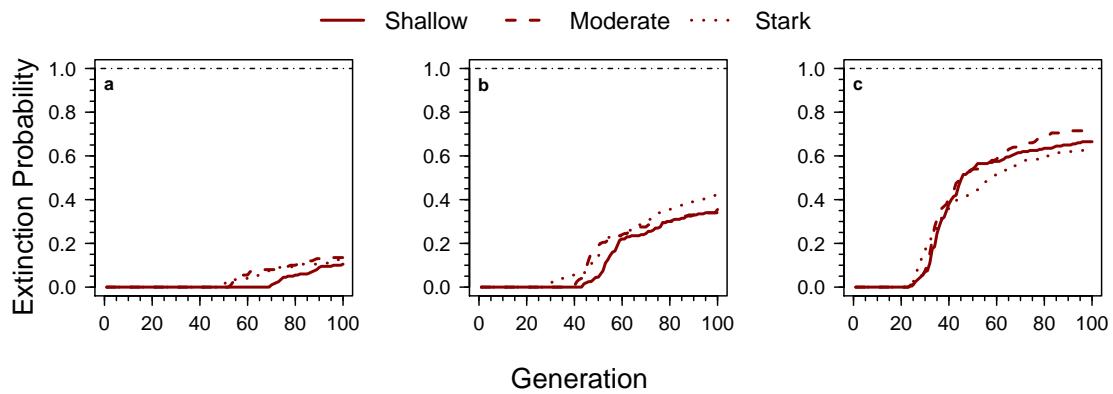


Figure B1: ~~Extinction probabilities for~~ The cumulative probability of extinction due to a slow speed of climate change in different experimental scenarios. Graphs show the proportion of simulated populations that went extinct through time for scenarios with a (a) ~~no flat~~, (b) ~~low shallow~~, and (c) ~~high potential for local adaptation~~ steep gradient in the niche optimum, and in environments ranges characterized by a shallow (solid line), moderate (dashed line), or stark (dotted line) ~~gradient at the range edge~~.

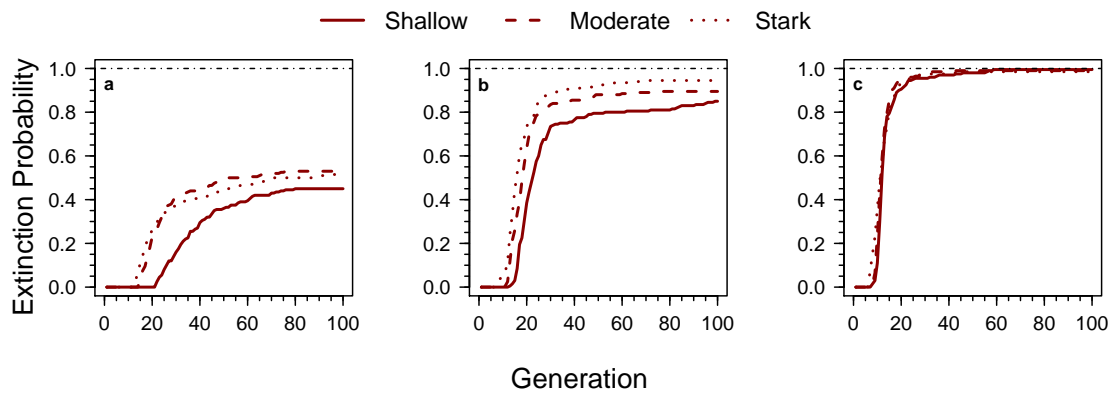


Figure B2: ~~Extinction probabilities for~~ The cumulative probability of extinction due to a fast speed of climate change in different experimental scenarios. Graphs show the proportion of simulated populations that went extinct through time for scenarios with a (a) ~~no~~ flat, (b) ~~low~~ shallow, and (c) ~~high potential for local adaptation~~ steep gradient in the niche optimum, and in environments ranges characterized by a shallow (solid line), moderate (dashed line), or stark (dotted line) gradient at the ~~range~~ edge.

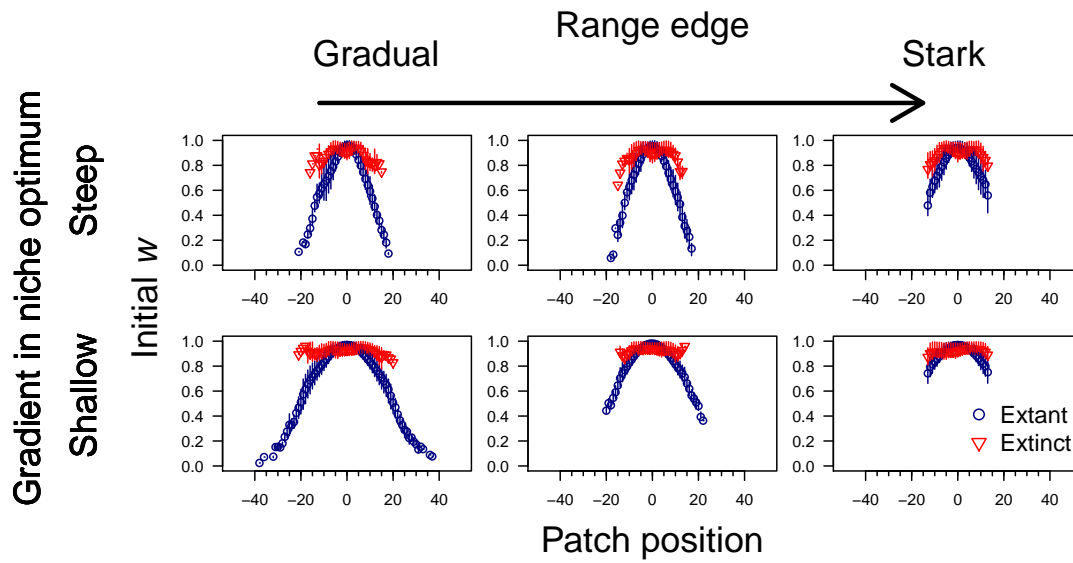


Figure B3: Individual fitness along the x ~~dimensions~~dimension of the landscape ~~prior to the onset of climate change~~at equilibrium. Points represent the mean across simulations and error bars are interquartile ranges. Population status (extinct or successful) was determined for a slow speed of climate change.

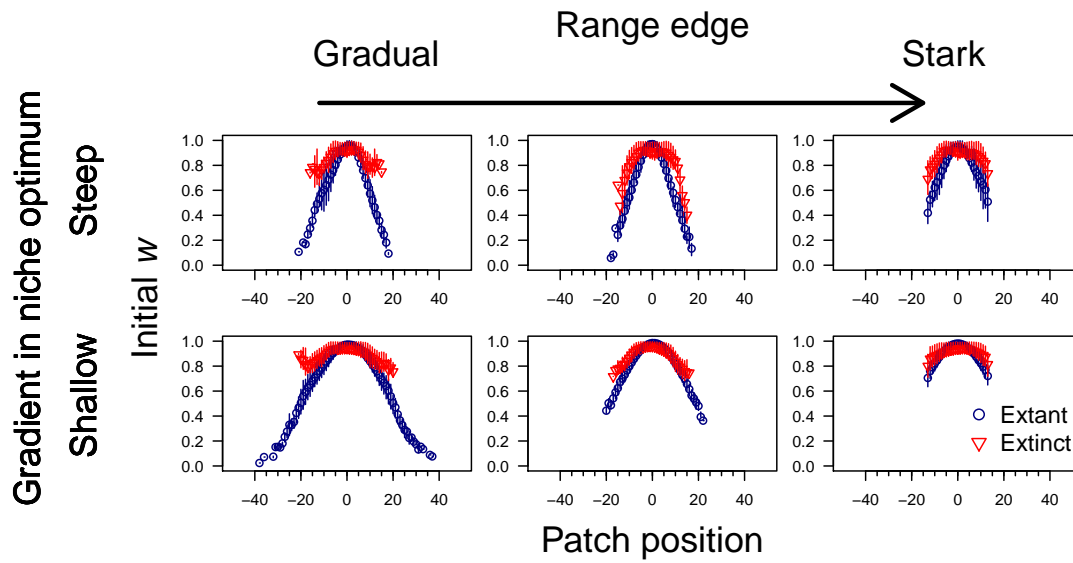


Figure B4: Individual fitness along the x ~~dimensions~~dimension of the landscape ~~prior to the onset of climate change~~at equilibrium. Points represent the mean across simulations and error bars are interquartile ranges. Population status (extinct or successful) was determined for a moderate speed of climate change.

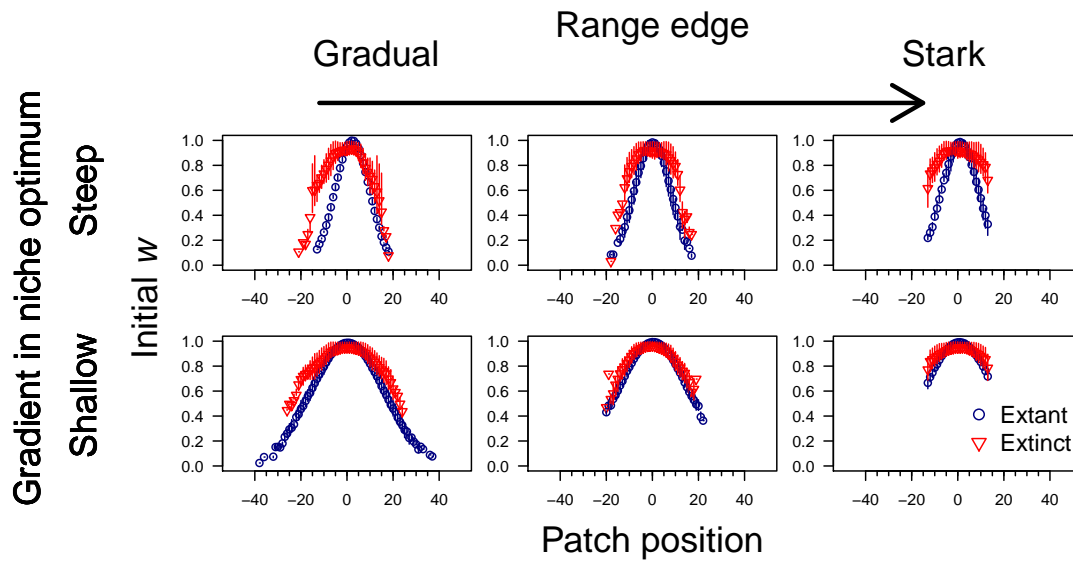


Figure B5: Individual fitness along the x ~~dimensions~~dimension of the landscape ~~prior to the onset of climate change~~at equilibrium. Points represent the mean across simulations and error bars are interquartile ranges. Population status (extinct or successful) was determined for a fast speed of climate change.

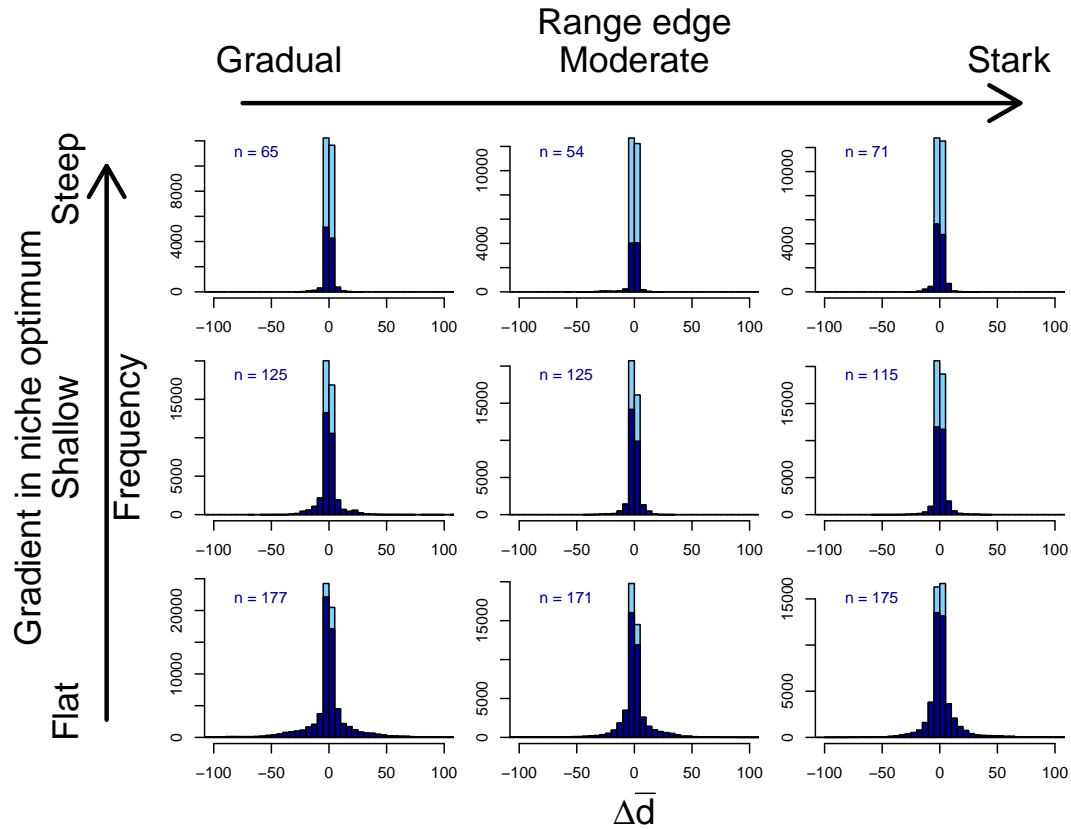


Figure B6: Observed dispersal evolution in populations responding to a slow speed of climate change. Positive values indicate an increase in average dispersal ability ~~over the course of~~ during climate change. The values ~~associate~~ associated with populations successfully tracking climate change are shown in dark blue and the total number of surviving populations is indicated in the top left corner. The experimental scenario corresponding to each histogram is indicated on the figure.

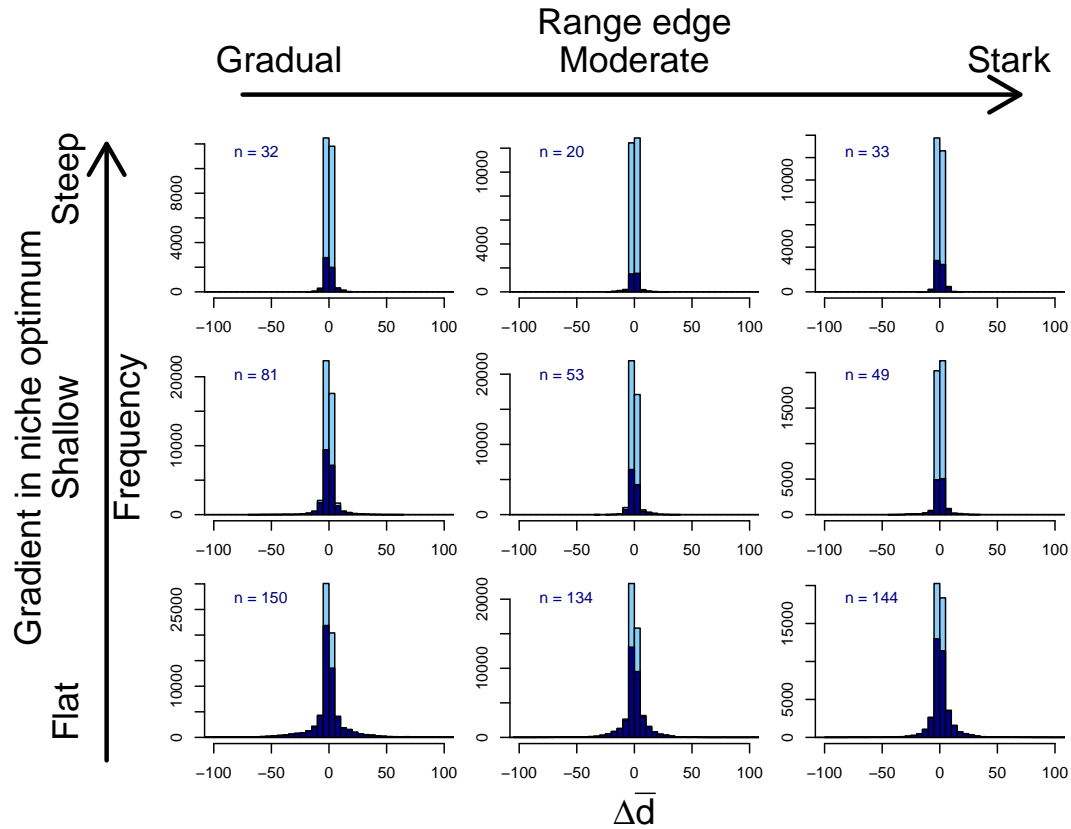


Figure B7: Observed dispersal evolution in populations responding to a moderate speed of climate change. Positive values indicate an increase in average dispersal ability ~~over the course of~~ during climate change. The values ~~associate~~ associated with populations successfully tracking climate change are shown in dark blue and the total number of surviving populations is indicated in the top left corner. The experimental scenario corresponding to each histogram is indicated on the figure.

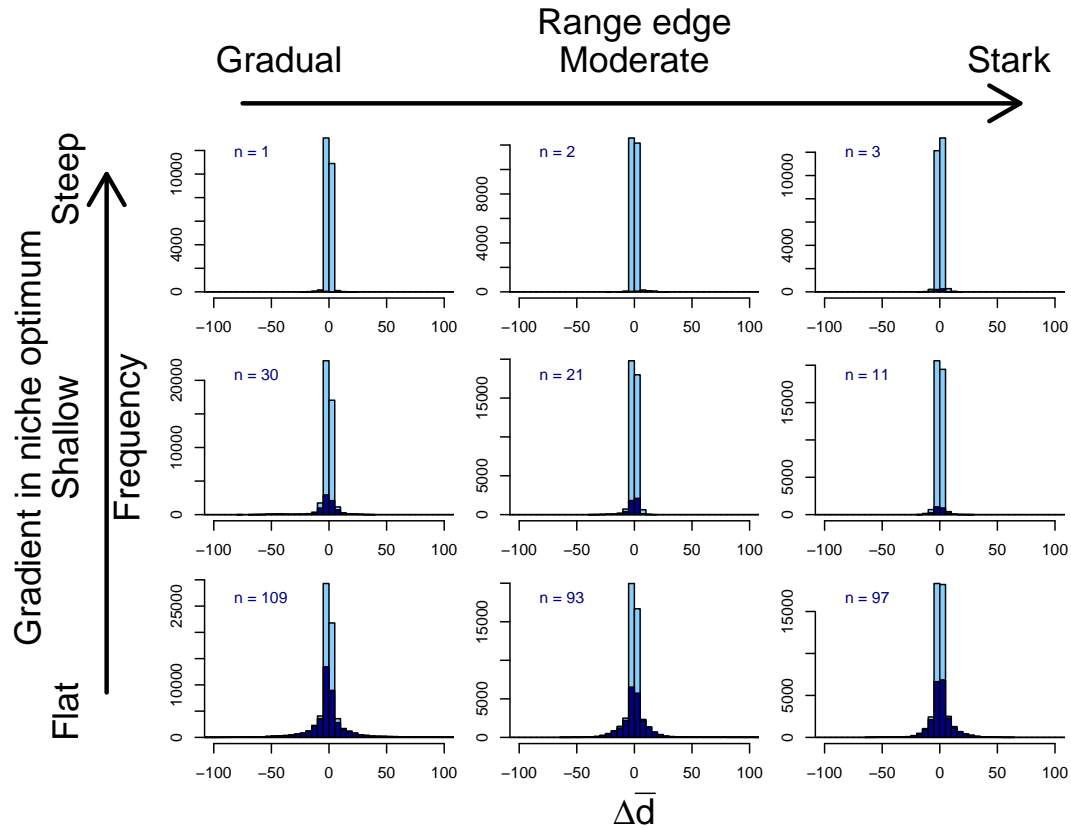


Figure B8: Observed dispersal evolution in populations responding to a fast speed of climate change. Positive values indicate an increase in average dispersal ability ~~over the course of~~ during climate change. The values ~~associate~~ associated with populations successfully tracking climate change are shown in dark blue and the total number of surviving populations is indicated in the top left corner. The experimental scenario corresponding to each histogram is indicated on the figure.

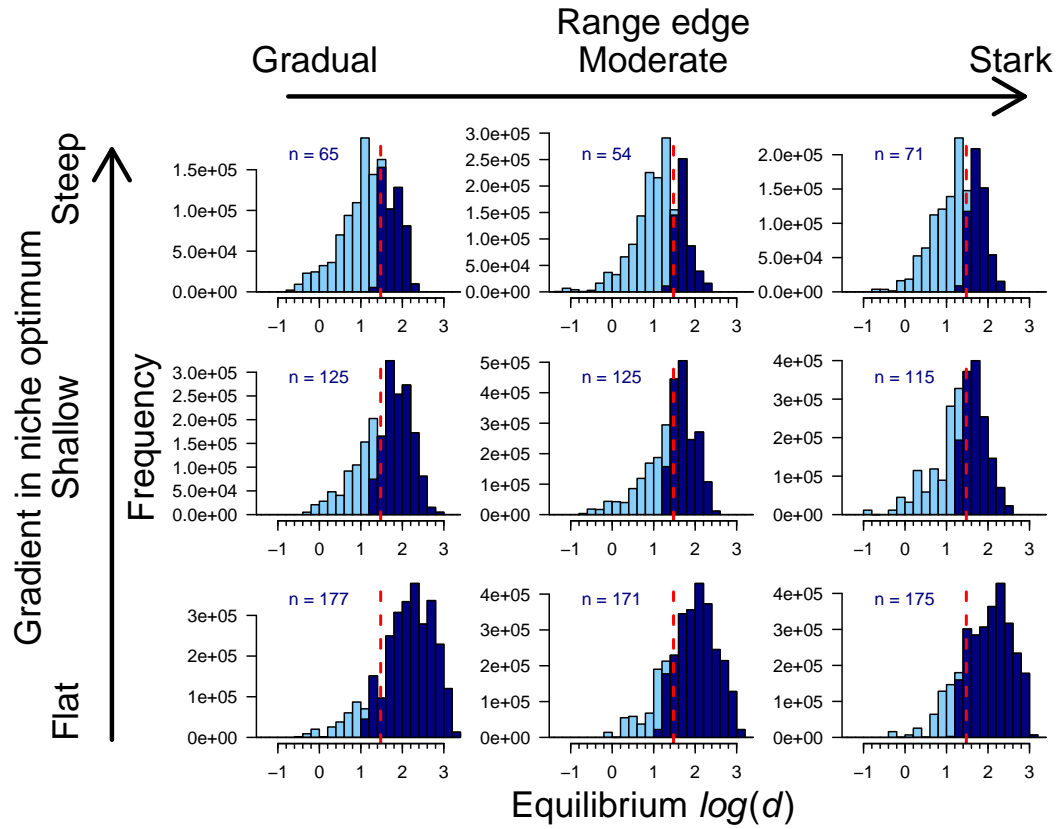


Figure B9: Distributions of the dispersal phenotypes observed in equilibrium populations ~~just prior to the onset of climate change~~. Phenotypes associated with populations that ultimately survived climate change are shown in dark blue and the total number of surviving populations is indicated in the top left corner. Vertical dashed lines indicate the dispersal phenotype necessary to produce an expansion wave exactly matching a slow speed of climate change.

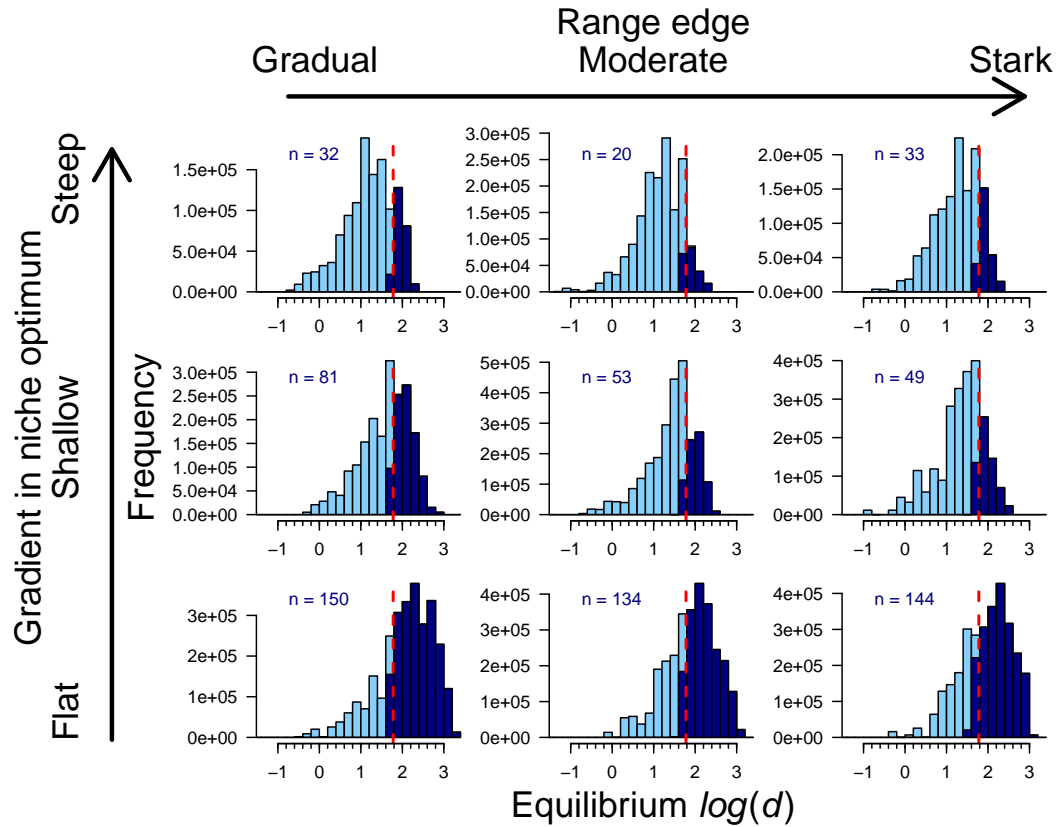


Figure B10: Distributions of the dispersal phenotypes observed in equilibrium populations ~~just prior to the onset of climate change~~. Phenotypes associated with populations that ultimately survived climate change are shown in dark blue and the total number of surviving populations is indicated in the top left corner. Vertical dashed lines indicate the dispersal phenotype necessary to produce an expansion wave exactly matching a moderate speed of climate change.

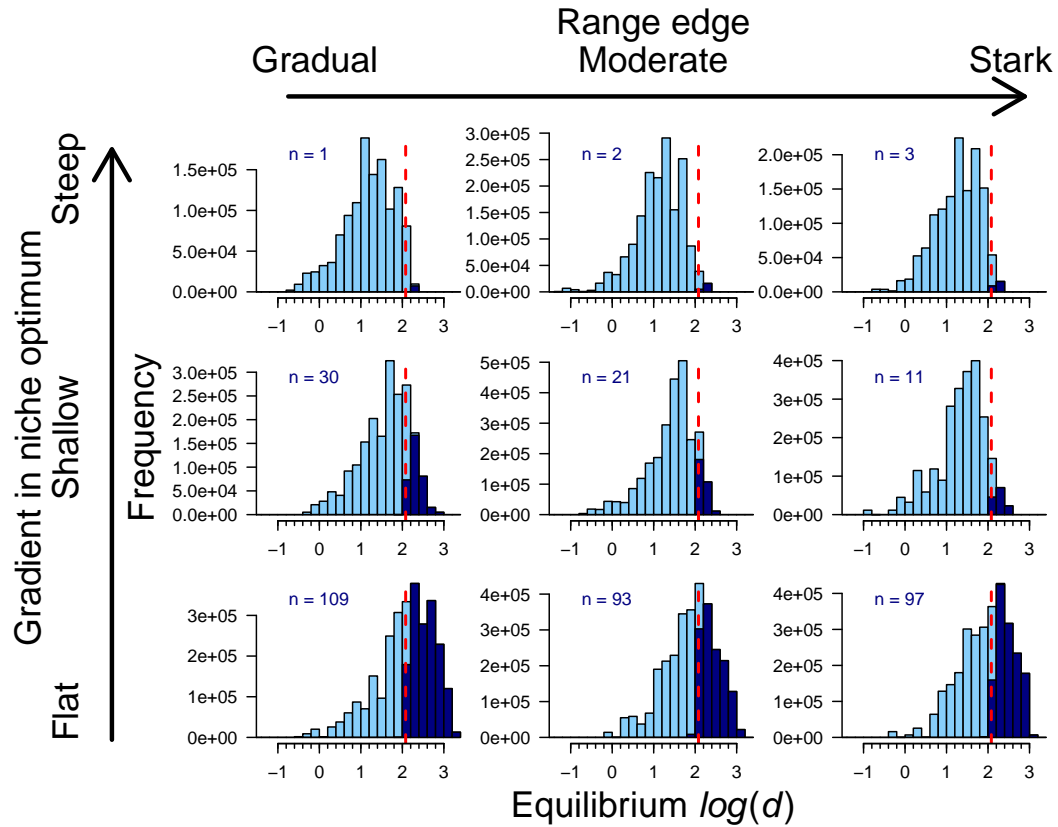


Figure B11: Distributions of the dispersal phenotypes observed in equilibrium populations ~~just prior to the onset of climate change~~. Phenotypes associated with populations that ultimately survived climate change are shown in dark blue and the total number of surviving populations is indicated in the top left corner. Vertical dashed lines indicate the dispersal phenotype necessary to produce an expansion wave exactly matching a fast speed of climate change.